



SCHOOL of
GRADUATE STUDIES
EAST TENNESSEE STATE UNIVERSITY

East Tennessee State University
**Digital Commons @ East
Tennessee State University**

Electronic Theses and Dissertations


Student Works

5-2017

Black Bears (*Ursus americanus*) versus Brown Bears (*U. arctos*): Combining Morphometrics and Niche Modeling to Differentiate Species and Predict Distributions Through Time

Theron Michael Kantelis
East Tennessee State University

Follow this and additional works at: <https://dc.etsu.edu/etd>

 Part of the [Other Environmental Sciences Commons](#), [Paleobiology Commons](#), and the [Paleontology Commons](#)

Recommended Citation

Kantelis, Theron Michael, "Black Bears (*Ursus americanus*) versus Brown Bears (*U. arctos*): Combining Morphometrics and Niche Modeling to Differentiate Species and Predict Distributions Through Time" (2017). *Electronic Theses and Dissertations*. Paper 3262. <https://dc.etsu.edu/etd/3262>

This Thesis - Open Access is brought to you for free and open access by the Student Works at Digital Commons @ East Tennessee State University. It has been accepted for inclusion in Electronic Theses and Dissertations by an authorized administrator of Digital Commons @ East Tennessee State University. For more information, please contact digilib@etsu.edu.

Black Bears (*Ursus americanus*) versus Brown Bears (*U. arctos*): Combining
Morphometrics and Niche Modeling to Differentiate Species and Predict Distributions
Through Time

A thesis
presented to
the faculty of the Department of Geosciences
East Tennessee State University

In partial fulfillment
of the requirements for the degree
Master of Science in Geosciences

by
Theron Michael Kantelis
May 2017

Dr. Blaine W. Schubert, Chair
Dr. Joshua Samuels
Dr. Chris Widga

Keywords: *Ursus arctos*, *Ursus americanus*, Bears, Geometric Morphometrics,
Ecological Niche Model, Teeth, Molars

ABSTRACT

Black Bears (*Ursus americanus*) versus Brown Bears (*U. arctos*): Combining
Morphometrics and Niche Modeling to Differentiate Species and Predict Distributions
Through Time
by

Theron Michael Kantelis

Late Pleistocene American black bears (*Ursus americanus*) often overlap in size with Pleistocene brown bears (*U. arctos*), occasionally making them difficult to diagnose. Large *U. americanus* have previously been distinguished from *U. arctos* by the length of the upper second molar (M2). However, the teeth of fossil *U. americanus* sometimes overlap size with *U. arctos*. As such, there is need for a more accurate tool to distinguish the two species. Here, 2D geometric morphometrics is applied to the occlusal surface of the M2 to further assess the utility of this tooth for distinguishing *U. americanus* and *U. arctos* specimens. When combined with an Ecological Niche Model of *U. americanus* and *U. arctos* in North America from the Last Glacial Maximum, this morphometric technique can be applied to key regions. A case of two Pleistocene specimens previously identified as *U. arctos* from eastern North America exemplifies the utility of this combination.

TABLE OF CONTENTS

	Page
ABSTRACT	2
LIST OF TABLES	4
LIST OF FIGURES	5
Chapter	
1. INTRODUCTION	6
2. GEOMETRIC MORPHOMETRIC ANALYSIS OF THE M2 OF <i>URSUS</i> <i>AMERICANUS</i> AND <i>U. ARCTOS</i>	12
Materials and Methods	12
Data Acquisition	12
Data Processing	17
Results	18
Principal Component Analysis	18
Discriminant Functions	21
Thin Plate Spline and Averaged Images	29
Discussion	33
Morphological Diagnosis	33
Further Implications	34
3. ECOLOGICAL NICHE MODEL OF <i>U. AMERICANUS</i> AND <i>U. ARCTOS</i> PROJECTED TO THE LAST GLACIAL MAXIMUM	37
Materials and Methods	38
Results	40
Discussion	50
4. CONCLUSIONS AND CASE STUDY	52
BIBLIOGRAPHY	63
APPENDIX	68
Additional Table and Figures	68

VITA 80

LIST OF TABLES

Table	Page
1. Landmark Descriptions and Placement.....	14
2. Total Variance Explained for Principal Component Analysis.....	19
3. Component Matrix for the Principal Component Analysis	22
4. Eigenvalues, Wilk's Lambda, and Classification Results.....	24
5. Stepwise Eigenvalues, Wilk's Lambda, and Classification Results	27
6. Total Variance Explained for the Case Study	
Principal Component Analysis	55
7. Component Matrix for the Case Study Principal Component Analysis.....	58
8. Eigenvalues, Wilk's Lambda, and Classification Results	
of the Case Study	59
9. Stepwise Eigenvalues, Wilk's Lambda, and Classification Results	
of the Case Study	61

LIST OF FIGURES

Figure	Page
1. Morphological Regions of the Upper Second Molar of <i>Ursus americanus</i> in Occlusal View	10
2. Visual Display of Landmark Locations.....	15
3. Scatter Plot of PC1 and PC2.....	20
4. Scatter Plot of PC1 and PC3.....	21
5. Histogram Plot of the Discriminant Function	25
6. Histogram Plot of the Stepwise Discriminant Function	28
7. Thin Plate Spline	30
8. Averaged Images of the M2 of <i>U. americanus</i> and <i>U. arctos</i>	31
9. Modern Ecological Niche Model for <i>U. americanus</i>	41
10. Modern Ecological Niche Model for <i>U. arctos</i>	42
11. Last Glacial Maximum Ecological Niche Model for <i>U. americanus</i>	43
12. Last Glacial Maximum Ecological Niche Model for <i>U. arctos</i>	44
13. Sensitivity vs. Specificity charts for the Ecological Niche Models.....	45
14. Comparison of the <i>U. americanus</i> Modern and LGM Ecological Niche Model	47
15. Comparison of the <i>U. arctos</i> Modern and LGM Ecological Niche Model	48
16. Area of significant presence (>.5) overlap between <i>U. americanus</i> and <i>U. arctos</i> at the LGM.....	49
17. Scatter Plot of the Case Study PC1 and PC2	56
18. Scatter Plot of the Case Study PC1 and PC3	57
19. Histogram Plot of the Case Study Discriminant Function.....	60
20. Histogram Plot of the Case Study Stepwise Discriminant Function.....	62

CHAPTER 1

INTRODUCTION

Numerous Pleistocene fossil sites across North America have reported specimens of *Ursus americanus* and *Ursus arctos* (Kurtén and Anderson, 1980; Graham and Lundelius 2010). Occasionally, these two species of bear are even found at the same fossil locality, and sometimes alongside other genera of bear such as *Arctodus* or *Tremarctos* (Kurtén and Anderson, 1980; Graham and Lundelius 2010). While neither *U. americanus* or *U. arctos* is easily mistaken for tremarctine bears, the majority of the differences between *U. americanus* and *U. arctos* may be difficult to assess in the fossil record (Gordon 1977, DeMaster and Stirling 1981, Graham 1991, Pasitschniak-Arts 1993, Larivière 2001). *Ursus arctos* is described as having a dished facial profile, significantly longer claws on the paws of the forelimbs than the hind limbs, an upper second molar (M2) length greater than 31 mm, a lower first molar (m1) length and width greater than 20.4 and 10.5 mm respectively, and a prominent shoulder hump, whilst *U. americanus* possess no such hump, has claws of nearly equal length on all paws, and has a more concave profile (DeMaster and Stirling 1981, Pasitschniak-Arts 1993, Larivière 2001). Aside from these features, modern *U. arctos* and *U. americanus* can be distinguished from each other by the larger size of *U. arctos* and often simply by the color of their pelage (DeMaster and Stirling 1981, Pasitschniak-Arts 1993, Larivière 2001). It should be noted, however, that while the common names of *U. arctos* and *U. americanus* imply a simple brown and black coloration respectively, *U. americanus* has been well documented to range widely in color (Pasitschniak-Arts 1993, Larivière 2001, DeMaster and Stirling 1981).

While this is a fair list of distinguishing features for living members of *U. arctos* and *U. americanus*, many of these characteristics are not necessarily applicable to fossil specimens. Coloration is not typically available in paleontology as the pelage is nearly always absent and is often discolored in the rare case of its preservation. The facial profile is difficult to distinguish without fleshy features and particularly if the skull is deformed or crushed. The shoulder hump present in *U. arctos* is not an osteological feature, so it does not readily preserve. Size is not necessarily reliable as studies have shown that Pleistocene and some Holocene *U. americanus* are able to achieve a size comparable to both modern and fossil members of *U. arctos* (Kurtén and Anderson 1980, Wolverton and Lyman 1998). In addition to a general size increase, the size of the teeth in Pleistocene *U. americanus* were also greater, making the use of molar length and width in identification difficult (Graham 1991). This leaves the length of the front and hind claws for the two species. In many cases, these elements are not discovered with the fossil specimen, so an identification must be made based on what is available (Elftman 1931, Kurtén 1963, Mustoe and Carlstad 1995, Czaplewski et al. 1999, Czaplewski and Willsey 2013, Czaplewski and Puckette 2014). These identifications are not made off of a defining character, but morphological similarity. As stated in several of these articles, this strategy is not preferable due to this technique leaving the identifications somewhat ambiguous.

As a result, there is a need for a greater number of diagnostic tools to identify these species in the fossil record. Preferably, this would be a method which does not rely on general morphological similarities. Due to the extreme level of general variability found in bears, it may require a larger number of specimens to accurately represent the

typical morphology of the species (Baryshnikov 2006). While the statement of extreme variability may sound extravagant, members of *U. arctos* alone have been attributed to upwards of 80 different species as well as several different genera (Pasitschniak-Arts 1993). While all of these have been synonymized with *U. arctos* or now refer to subspecies, this exemplifies how the variability within *Ursus* can cause confusion in identification. Also, there is a precedent set for misidentified specimens. In 1991, Graham suggested the reassignment of several Pleistocene *Ursus* due to misunderstandings of how large *U. americanus* could be during that time period. These specimens had been assigned to *U. arctos* based on their size, as no modern *U. americanus* have reached that size. Despite the variation in *Ursus*, length and width measurements of the molars has shown to be one of the most effective ways to identify a specimen, fossil or otherwise (Graham 1991). Therefore, if a method is required to better identify specimens, it logically would originate at the molars.

Gordon (1977) showed that modern *U. arctos* and *U. americanus* could be distinguished by the length and width of m1 and M2. The length and width of the m1 had a 100 percent success rate in identifying the species and the length of the M2 had 95 and 100 percent success rate for the two species, respectively. Gordon used between 51 and 144 specimens for each of these measurements, but neglected to mention where these specimens were sourced from. While Gordon tested other measurements of the teeth, these were either significantly less successful in one or both species, or were shown to be inconsistent by Graham in 1991. Between the m1 and M2, the M2 is the more common of the teeth due to its size and connection to skull rather than the mandible. As such, the M2 is the tooth of choice in this study. Length and width

measurements of the teeth have shown to be somewhat ineffective due to an overlap in size between Pleistocene *U. americanus* and *U. arctos* (Kurtén and Anderson 1980). As such, a geometric morphometric study would be preferred to a study of linear measurements; though there are complications. As previously stated, bears generally have a high degree of variability. Within *U. arctos* and *U. americanus*, the number of premolars is variable, and even between the left and right and maxillary and mandibular premolars (Graham 1991, Baryshnikov et al. 2003, Baryshnikov 2006, Baryshnikov 2007). Gordon (1977) and Graham (1991) attempted to test the presence of accessory cusps on the p4, m1, and P4, but were met with widely disparate success rates.

Dental terminology here follows to Baryshnikov (2007) “for describing the ursine M2. The different cusps and areas of a typical ursine M2 are detailed in Figure 1.

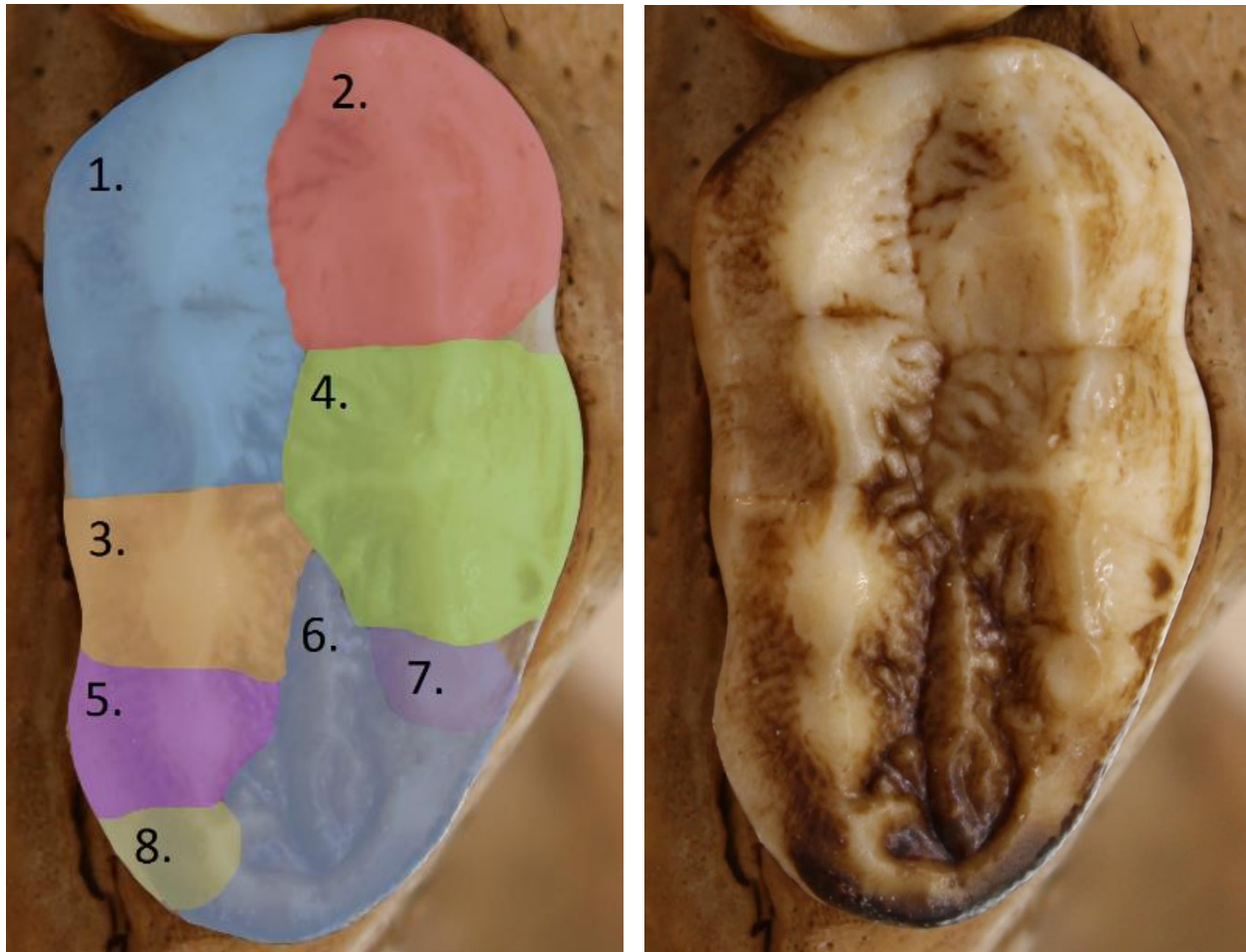


Figure 1. Morphological Regions of the Upper Second Molar of *Ursus americanus* in Occlusal View (ETVP 18252; left M2 shown). 1) Protocone, 2) Paracone, 3) Metaconule, 4) Metacone, 5) Hypocone, 6) Talon, 7) Post-Metacone Accessory Cusp (not always present), 8) Post-Hypocone Accessory Cusp (not always present). The shapes of these regions may be inconsistent between individuals and species, but their relative positions are consistent outside of pathologies.

Development of a technique for differentiating the M2 of *U. arctos* and *U. americanus* is one aspect of this project. *Ursus* occurs throughout the majority of North America, and fossil specimens from the Pleistocene appear to have been present within a quite different range from that of modern times. (Pasitschniak-Arts 1993, Larivière 2001, Graham and Lundelius 2010). To better predict what species of *Ursus* would be found at a particular locale, this study also creates an ecological niche model of where

U. arctos and *U. americanus* are expected to have been present during the Last Glacial Maximum (LGM). By using modern bioclimatic variables to understand the habitat preferences of these species, bioclimatic variables from the LGM can be used to approximate the LGM range. This may help in identifying specimens whose identification should be reassessed. Specimens occurring significantly outside of their expected range could represent misidentification, or, if they were correctly identified, a substantial difference between the environmental preferences of *Ursus* species between the Pleistocene and now. There are periods of the Pleistocene which were different ecologically from today and the LGM, so this model cannot be perfect, but this model will give a general idea of where the species could have been present given the general climatic differences between the Pleistocene and present. As there are fossil specimens of that have been described as *U. arctos* that are well outside of their modern historic range, this aspect of the study should help to determine how unusual or expected that expanded range is (Graham and Lundelius 2010).

CHAPTER 2

GEOMETRIC MORPHOMETRIC ANALYSIS OF THE M2 OF *URSUS AMERICANUS* AND *U. ARCTOS*

Materials and Methods

Data Acquisition

For the analysis, 64 (34 *U. americanus*, 30 *U. arctos*) modern specimens (collected within the past 150 years) were collected from two collections, the East Tennessee State University comparative collection (ETVP) and the National Museum of Natural History's (NMNH) mammal collection. From the ETVP, *U. americanus* specimens are largely from Tennessee, and *U. arctos* are largely from Alaska, with several belonging to *U. a. middendorffi*, the Kodiak subspecies. From the NMNH collection, specimens originate from the entirety of the modern historic range. Specimen numbers, and their origins can be seen in Appendix A (pg 64). The choice of specimens for this study attempts to mimic and therefore account for any regional geographic variation that might otherwise skew the results. This said, there aren't any specimens in the sample that represent regions outside North America. The inclusion of such specimens could have given the results a "Eurasian" skew, and not accurately represented the differences between bears that might have actually occurred in the same region (Taberlet and Bouvet 1994).

The ETVP collection *Ursus* collection is limited in geographic scope, and most available specimens were used that had complete M2's with well-preserved cusps. Because of the vast collection at the NMNH, specimen choice focused on those with teeth in the best condition. Complete and relatively unworn were preferred, with careful

attention made to not disregard teeth that appeared to have an unusual shape or morphology (not to be confused with those bearing a pathology). While such teeth might be considered potential outliers in studies of most animals, bear teeth are well documented to be highly variable (Baryshnikov 2007), so this line of thought could potentially create a bias towards overly homologous teeth, when in reality, many teeth of relatively strange or unusual shape may need to be identified by the results of this study (Baryshnikov 2006).

Data acquisition consisted of photographs taken perpendicular to the palate, such that the lens of the camera was parallel with the flat surface of the palate. Future studies might use 3D landmarks (e.g., using a microscribe), but care will need to be taken in landmark choice, as wear on the teeth could invalidate some of the landmarks chosen here. That said, 3D landmarks remove the concern of photograph orientation, so there are definite benefits to this strategy.

Table 1. Landmark Descriptions and Placement. See Figure 2 for a visual representation of the placement of these landmarks.

Landmark	Description
1	Point of maximum curvature on labial side of the paracone
2	Point of minimum curvature on labial side between the paracone and metacone
3	Point of maximum curvature on labial side of the metacone
4	Point of maximum curvature on posterior end of tooth
5	Point of maximum curvature on lingual side of the anterior portion of lingual cingulum
6	Most anterior tip of the paracone
7	Apex of paracone
8	Intersection of paracone and metacone blades
9	Apex of metacone
10	Most posterior end of the metacone
11	Point of maximum curvature on lingual side of the metacone
12	Intersection of the paracone, metacone, and protocone
13	Intersection of the protocone, metaconule, and metacone.

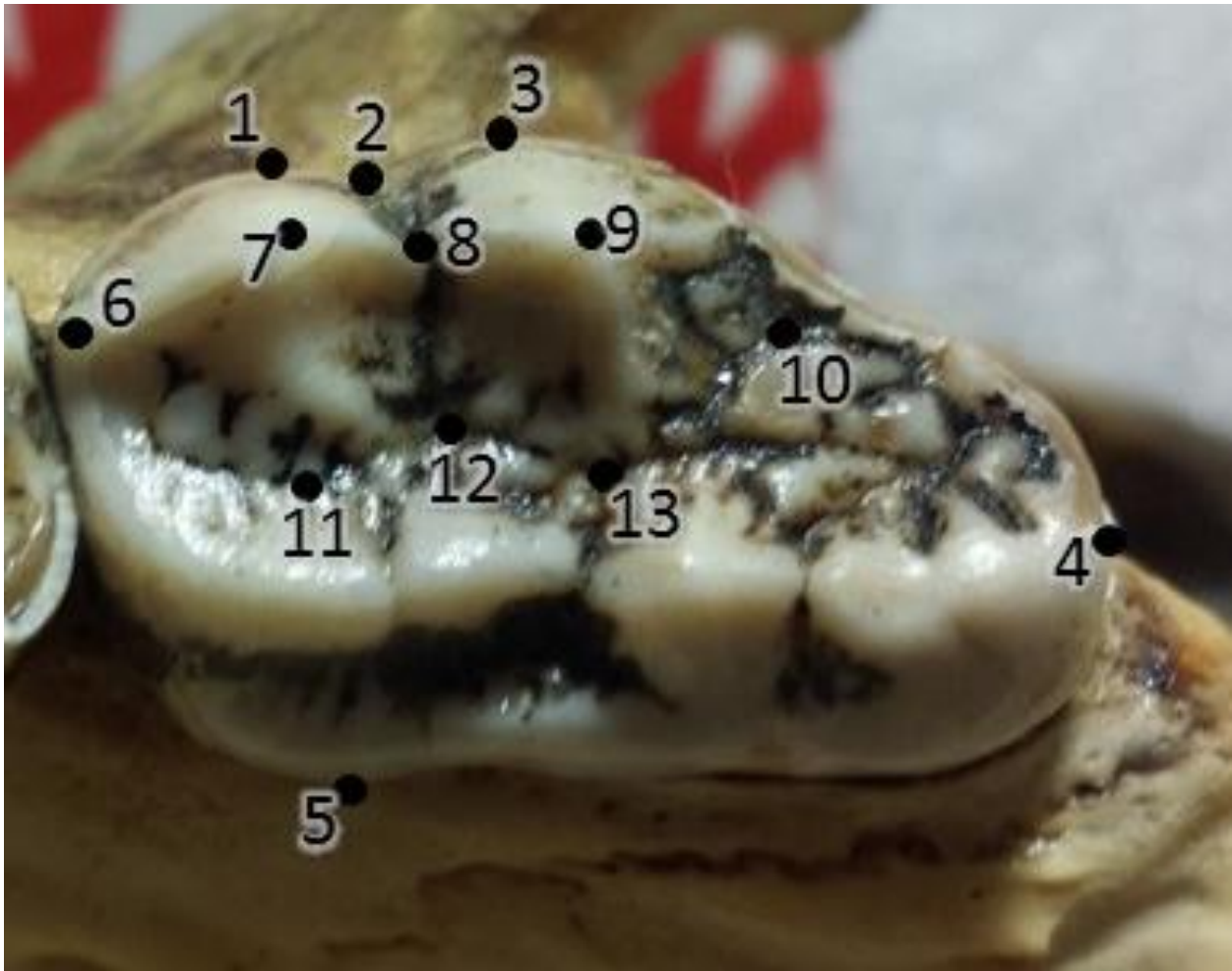


Figure 2. Visual Display of Landmark Locations. USNM 227660 (U. americanus) displaying the locations of the thirteen landmarks used in this study.

As previously mentioned, landmarks were chosen based on consistency and ability to be recognized, as such, all landmarks chosen are type 1 and type 2 (Bookstein 1991). Sliding landmarks and type 3 landmarks were avoided due to concerns of consistency within each species (Bookstein 1991). The landmarks chosen are listed and shown in Table 1, and Figure 2, respectively. Landmarks 1-6 were chosen to represent the recognizable and consistent locations on the exterior outline of the tooth, these being the widest point of the paracone, narrowest point between the paracone and metacone, widest point at the metacone, the most posterior, most lingual, and most anterior tips respectively. Landmarks 7 and 9 were chosen as they are the only cusp apices which are consistently recognizable, as all lingual side cusp apices are difficult to consistently recognize with a strong level of certainty. Only 35 of the 63 specimens (53.84%) would have been able to have additional landmarks placed along the lingual side cusps. The remaining specimens all had one or more potential landmark that could not be confidently identified. The protocone long, ridgelike, and often split, obscuring or duplicating the apex; the metaconule is reduced in *U. americanus*; the hypocone is often reduced in *U. americanus*; and the post hypocone is often absent or highly reduced in *U. arctos*. Landmark 8 and 10 were chosen to represent the boundaries of the paracone and metacone alongside landmark 6. Landmarks 11-13 were chosen to flesh out the remaining boundaries for the paracone and metacone, but also acted as proxies for the size and location of the lingual cusps.

Data Processing

After photographs were taken, they were compiled into a TPS file using tpsUtil64 (Version 1.74), part of the “tps” series of programs developed by F. James Rohlf (2015). This was done once for the teeth from ETSU, once for the teeth from NMNH, once to encompass both of them. From here, photographs had landmarks placed on them using tpsDIG2w32 software (Version 2.30) (Rohlf 2015). Any tooth whose landmarks could not be confidently assessed during the landmarking process was removed from the study. Once landmarked, the image sets had their consensus configuration determined through tpsRelw32 (Version 1.67) (Rohlf 2015). The aligned landmark data was saved from the consensus. After the aligned landmark data was saved, it was formatted using Microsoft Office Excel such that it was in a format applicable in the SPSS statistical package. Within SPSS, a trio of analyses were performed for each group of specimens: A Principal Component Analysis (PCA), a Discriminant Analysis, and a Step-Wise Discriminant Analysis. Deformation grids were added to the plots of the analyses for the sake of representing the shape differences along the axes. These deformation grids were generated by placing the principal component scores and discriminant function scores in a .nts file for use within tpsRegr (Version 1.42) (Rohlf 2015).

In addition, a copy of the data file for specimens from the NMNH was split into *U. americanus* and *U. arctos* files, from which unwarped and averaged images were created in the tpsSuper (Version 2.03) and saved (Rohlf 2015). The averaged images hold no real statistical significance, but they do help to provide a visual representation of the differences between the two species. A thin-plate spline was also generated from

the NMNH specimens using the aligned *U. americanus* and *U. arctos* data from the averaged images in tpsSpline (Version 1.22) (Rohlf 2015).

Results

Principal Component Analysis

The results from the principal component analysis consisted of eight principal components scoring an eigen value of greater than 1, with the top three principal components representing 50% of the cumulative variance at 27.867%, 12.851%, and 9.520%. As the first 3 principal components represent 50% of the variance total, and proceeding components represent less than 10% of the variance each, scatter plots were only generated for the first three principal components. As is described below, principal components two and three appear to be showing within species variation, so they were not plotted against each other. Data for these and the remaining principal components can be seen in Table 2. A scatter plot of the first and second principal components can be seen in Figure 3, and a plot of the first and third principal components can be seen in Figure 4.

The first principal component appears to be expressing an elongation of the tooth in *U. arctos* and an expansion of the lingual cusps, though the space between the intersection of the paracone metacone and protocone and the intersection of the protocone, metaconule, and metacone are is much smaller. An elongation of the tooth in *U. arctos* is not surprising considering the usefulness of that measurement in modern specimens (Gordon 1977, Graham 1991). The second principal component appears to show variation of the relative position of the cusp apices within each species as it does

not show any strong variation between the species. The third principal component appears to show variation of the length of the posterior portion of the metacone within each species without any strong variation between species. The component matrix in Table 3 shows the scores for these and the remaining components.

Table 2. Total Variance Explained for Principal Component Analysis

Component	Initial Eigenvalues			Extraction Sums of Squared Loadings		
	Total	% of Variance	Cumulative %	Total	% of Variance	Cumulative %
1	7.245	27.867	27.867	7.245	27.867	27.867
2	3.341	12.851	40.718	3.341	12.851	40.718
3	2.475	9.520	50.238	2.475	9.520	50.238
4	2.108	8.107	58.345	2.108	8.107	58.345
5	1.891	7.273	65.618	1.891	7.273	65.618
6	1.458	5.607	71.225	1.458	5.607	71.225
7	1.266	4.870	76.095	1.266	4.870	76.095
8	1.070	4.116	80.211	1.070	4.116	80.211
9	.966	3.716	83.927			
10	.621	2.390	86.318			
11	.603	2.321	88.639			
12	.540	2.075	90.714			
13	.485	1.864	92.578			
14	.400	1.538	94.116			
15	.346	1.329	95.445			
16	.293	1.128	96.573			
17	.273	1.050	97.623			
18	.205	.788	98.411			
19	.169	.650	99.061			
20	.120	.460	99.521			
21	.070	.270	99.791			
22	.054	.208	99.999			
23	.000	.000	99.999			
24	8.757E-005	.000	100.000			
25	6.532E-005	.000	100.000			
26	2.966E-005	.000	100.000			

Extraction Method: Principal Component Analysis.

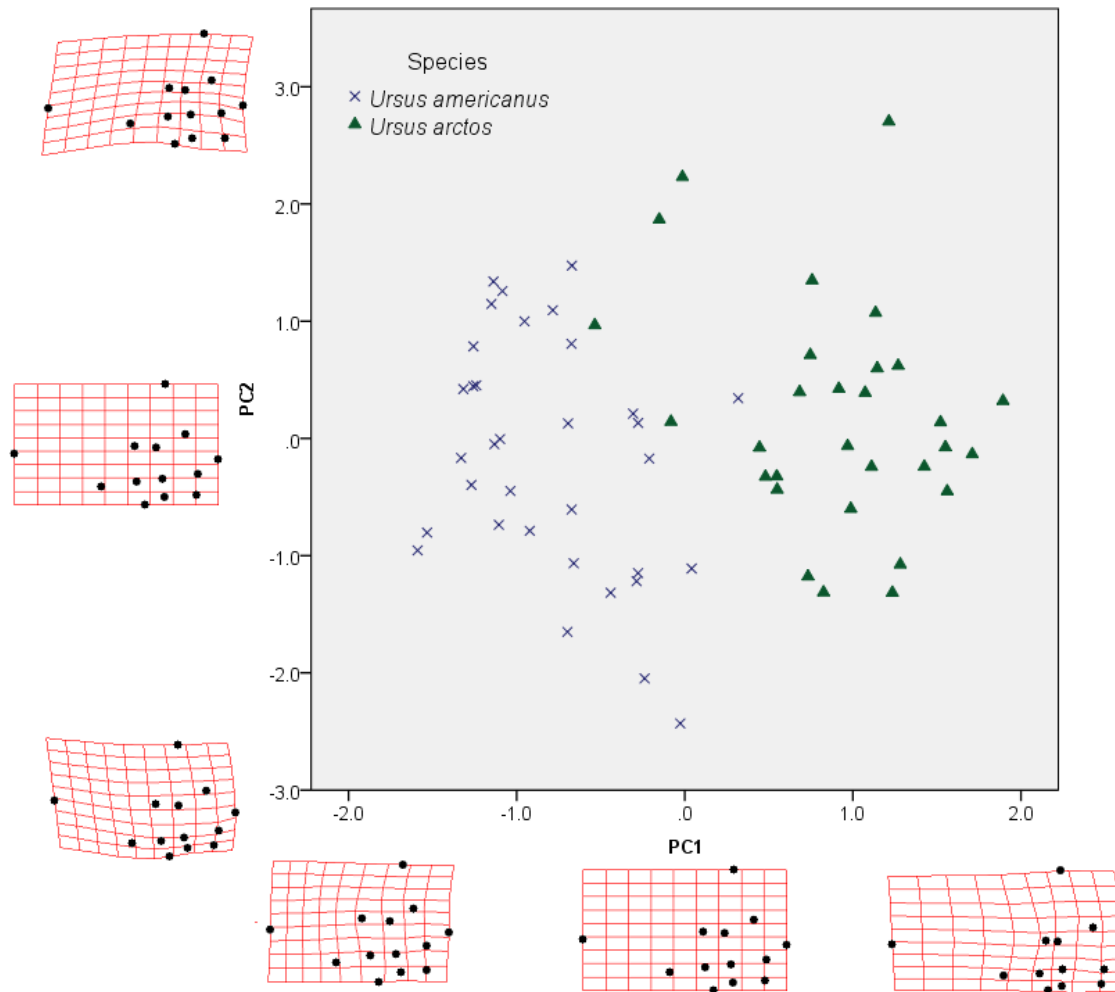


Figure 3. Scatter Plot of PC1 and PC2. The first principal component shows lateral compression or extension with an inverse effect along the anterior landmarks. The second principal component shows a vertical bending of the anterior landmarks of the tooth.

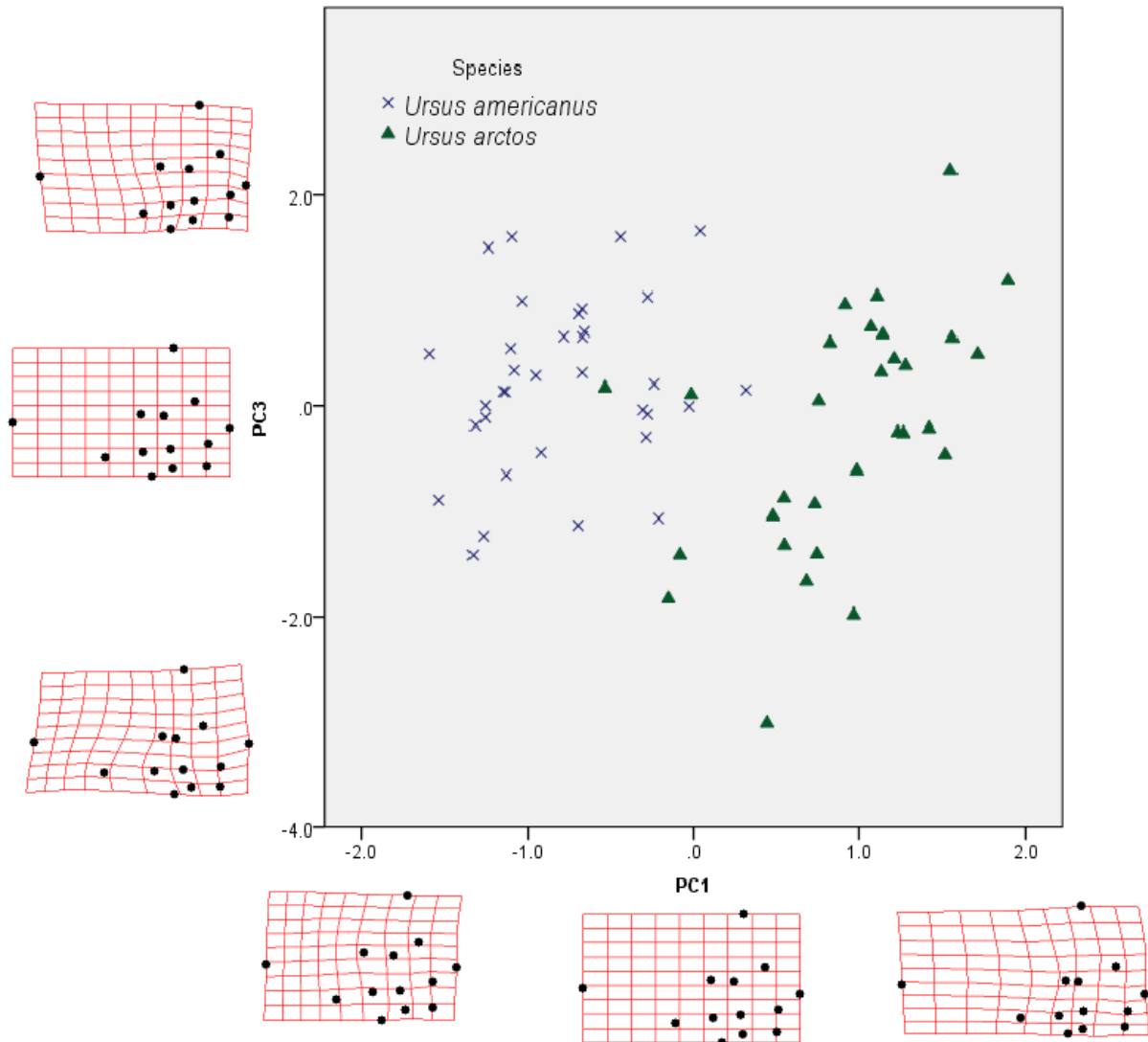


Figure 4. Scatter Plot of PC1 and PC3. The first principal component shows lateral compression or extension with an inverse effect along the anterior landmarks. The third principal component shows a twisting such that the lingual and labial sides of the middle of the tooth inversely compress or expand.

Table 3. Component Matrix for the Principal Component Analysis

Component Matrix^a

	Component							
	1	2	3	4	5	6	7	8
X1	.179	.044	.019	-.711	-.321	-.057	.284	-.073
X2	-.507	-.169	-.437	-.059	.393	-.040	.328	.182
X3	.452	-.066	-.635	-.024	.321	-.222	.080	-.030
X4	-.844	-.336	-.200	.028	-.261	.131	-.006	.018
X5	-.481	.522	.140	-.361	.216	-.331	-.017	.059
X6	-.474	-.129	-.502	.185	-.390	.133	-.021	-.175
X7	.116	-.265	.120	.366	-.151	.516	.309	-.378
X8	-.139	.153	.188	.630	.447	.102	.193	.044
X9	.411	.185	.283	.236	.514	.052	-.186	-.221
X10	.392	-.128	.628	-.040	.091	-.204	-.149	-.289
X11	.334	-.162	.359	-.218	-.255	.520	-.394	.274
X12	-.091	.006	.254	.499	-.067	.064	.224	.686
X13	.726	.239	-.308	.144	-.142	-.170	-.118	.143
Y1	.671	-.372	.113	-.246	.196	-.130	.357	.107
Y2	.840	-.100	.124	.005	-.232	-.162	.124	.179
Y3	.901	.065	.011	.047	-.205	-.084	-.017	.051
Y4	.282	-.796	.052	-.087	.280	.152	.180	-.158
Y5	-.026	-.538	-.074	.371	-.216	-.368	-.424	.035
Y6	-.343	-.335	-.328	-.358	.326	.330	-.379	.174
Y7	-.593	.385	.236	-.338	.280	.255	-.029	.095
Y8	.308	.760	.083	.030	.064	.274	-.024	-.040
Y9	-.020	.711	-.125	.053	-.429	.100	.254	-.087
Y10	.316	.443	-.630	.186	.137	.131	-.160	-.093
Y11	-.773	-.187	.216	.034	-.156	-.119	.195	-.059
Y12	-.758	.156	.185	.184	-.046	-.344	-.177	-.140
Y13	-.836	.046	.241	.058	-.047	-.130	.044	.022

Extraction Method: Principal Component Analysis.

a. 8 components extracted.

Discriminant Functions

The discriminant function analysis resulted in a high eigenvalue of 8.736 and a .103 Wilk's lambda. These indicate that large proportion of the variance is explained by the discriminant function and that the two species have very low variability within their groups compared to the variability between each other. Eigenvalues, Wilk's lambda, and Classification results can be seen in Table 4. The discriminant function showed a 94.1% success rate at identifying *U. americanus*, and a 93.3% success rate at identifying *U. arctos*. Further inspection of the misidentified individuals suggests that one of the misidentified specimens (ETVP 5162) may actually be identified within the collection incorrectly, thus increasing the *U. arctos* identification success rate to 96.6%. Images of the misidentified teeth, as well as the Casewise Statistics can be found in Appendix A. The Histogram plot of the discriminant function can be seen in Figure 5. The discriminant function appears to be representing the same shape variation as seen in the first principal component

Table 4. Eigenvalues (Top), Wilk's Lambda (Middle), and Classification Results (Bottom). Classification results show a strong level of accuracy, and helped to reveal one possibly incorrectly identified specimen.

Eigenvalues

Function	Eigenvalue	% of Variance	Cumulative %	Canonical Correlation
1	8.736 ^a	100.0	100.0	.947

a. First 1 canonical discriminant functions were used in the analysis.

Wilks' Lambda

Test of Function(s)	Wilks' Lambda	Chi-square	df	Sig.
1	.103	116.067	22	.000

Classification Results^{a,c}

			Predicted Group Membership		Total
			1	2	
Original	Count	1	34	0	34
		2	0	30	30
	%	1	100.0	.0	100.0
		2	.0	100.0	100.0
Cross-validated ^b	Count	1	32	2	34
		2	2	28	30
	%	1	94.1	5.9	100.0
		2	6.7	93.3	100.0

a. 100.0% of original grouped cases correctly classified.

b. Cross validation is done only for those cases in the analysis. In cross validation, each case is classified by the functions derived from all cases other than that case.

c. 93.8% of cross-validated grouped cases correctly classified.

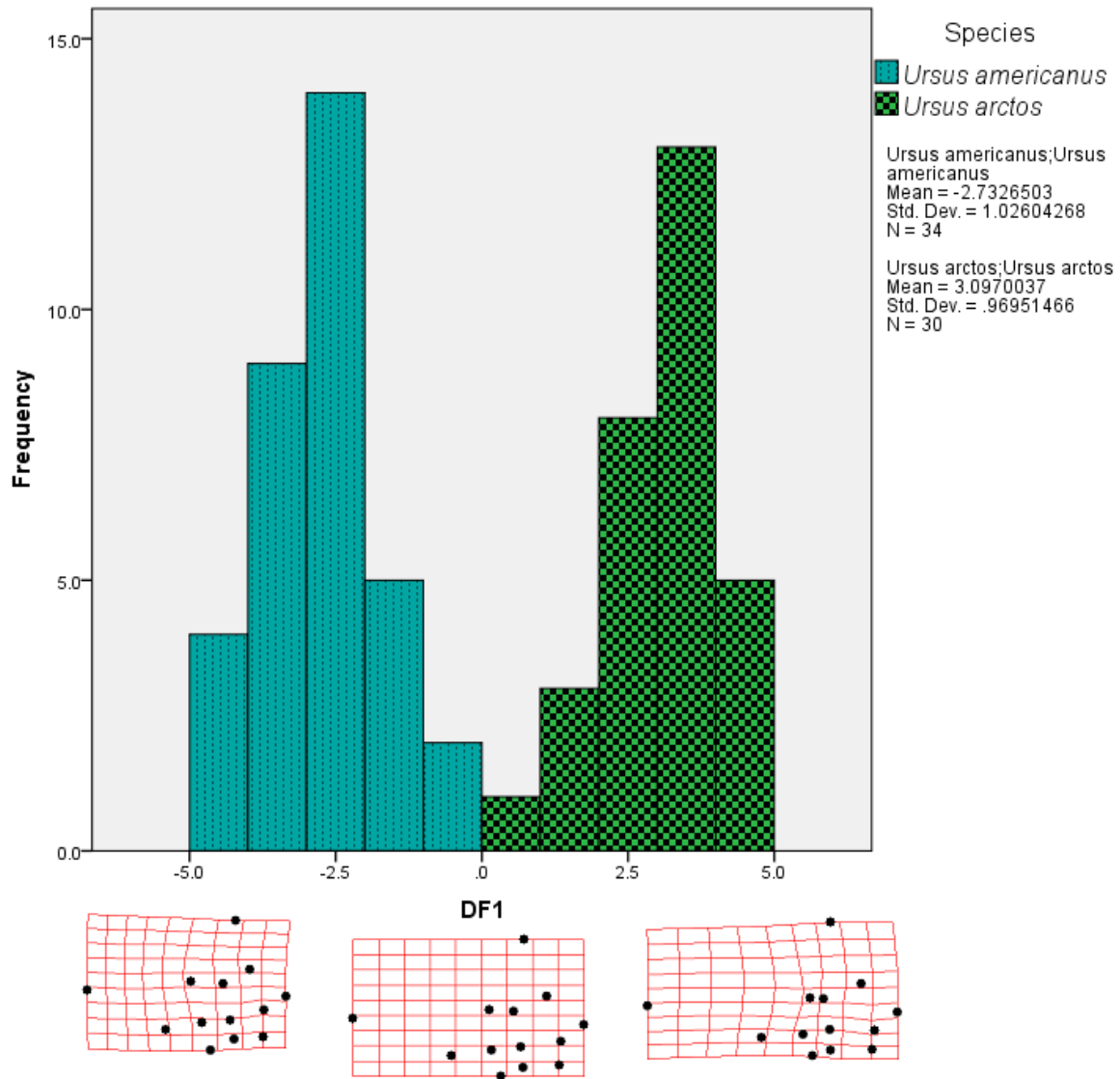


Figure 5. Histogram Plot of the Discriminant Function. The discriminant function represents the same variation as the first principal component.

Much like the discriminant function, the stepwise discriminant function analysis resulted in a high, though lower than the discriminant function's, eigenvalue of 5.059 and a low, though higher than the discriminant function's, .103 Wilk's lambda. The stepwise discriminant specified variables Y3, Y10, Y13, Y8, and X6 as being particularly valuable in discrimination. These variables, with the exception of X6 appear to be clustered around the metacone and metaconule, suggesting that these cusps might be important in distinguishing the teeth of the two species. Variables Entered, Eigenvalues, Wilk's lambda, and Classification results can be seen in Table 4. While the discriminant function misidentified some specimens, the stepwise discriminant function had zero misidentifications. This said, with ETVP 5162 potentially being misidentified within the collection, the success rate of *U. arctos* identification remains at 96.66%. Casewise Statistics can be found in Appendix A. The Histogram plot of the stepwise discriminant function can be seen in Figure 6. The stepwise discriminant function appears to be representing very similar shape variation as the discriminant function, though with more expansion and contraction in the posterior half of the tooth.

Table 5. Stepwise Eigenvalues (Top), Wilk's Lambda (Middle), and Classification Results (Bottom). Classification results show a strong level of accuracy, though the presence of a possibly misidentified specimen within the collection lowers the accuracy of U. arctos identification to 96.66%.

Eigenvalues

Function	Eigenvalue	% of Variance	Cumulative %	Canonical Correlation
1	5.059 ^a	100.0	100.0	.914

a. First 1 canonical discriminant functions were used in the analysis.

Variables Entered/Removed^{a,b,c,d}

Step	Entered	Wilks' Lambda							
		Statistic	df1	df2	df3	Exact F			
						Statistic	df1	df2	Sig.
1	Y3	.309	1	1	62.000	138.639	1	62.000	.000
2	Y10	.236	2	1	62.000	98.952	2	61.000	.000
3	Y13	.203	3	1	62.000	78.318	3	60.000	.000
4	Y8	.181	4	1	62.000	66.849	4	59.000	.000
5	X6	.165	5	1	62.000	58.689	5	58.000	.000

At each step, the variable that minimizes the overall Wilks' Lambda is entered.

- a. Maximum number of steps is 52.
- b. Minimum partial F to enter is 3.84.
- c. Maximum partial F to remove is 2.71.
- d. F level, tolerance, or VIN insufficient for further computation.

Classification Results^{a,c}

	ID	Predicted Group Membership		Total	
		1	2		
Original	Count	1	34	34	
		2	0	30	
	%	1	100.0	.0	100.0
		2	.0	100.0	100.0
Cross-validated ^b	Count	1	34	34	
		2	0	30	
	%	1	100.0	.0	100.0
		2	.0	100.0	100.0

- a. 100.0% of original grouped cases correctly classified.
- b. Cross validation is done only for those cases in the analysis. In cross validation, each case is classified by the functions derived from all cases other than that case.
- c. 100.0% of cross-validated grouped cases correctly classified.

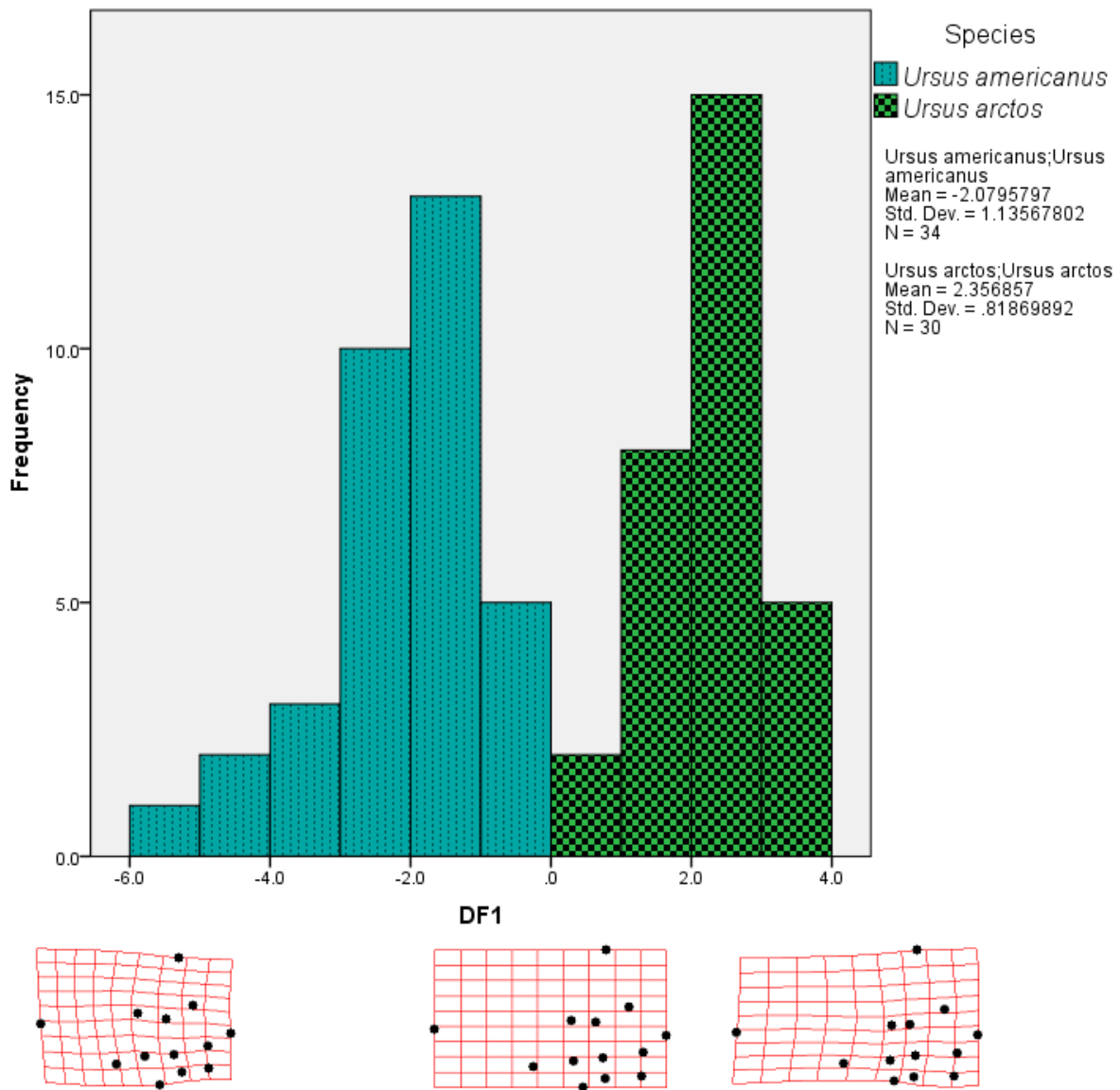


Figure 6. Histogram Plot of the Stepwise Discriminant Function. The stepwise discriminant function represents very similar variation as the discriminant function.

Thin Plate Spline and Averaged Images

The thin plate spline (Figure 7) shows several prominent differences between the M2 of the two species. In relation to *U. americanus*, *U. arctos* does have a longer tooth, as has been stated previously, but there are other prominent differences. This includes the following characters for *U. arctos* that distinguish it from *U. americanus*: paracone and metacone have much longer blades on the posterior side; widest point of the metacone on the labial side is shifted anteriorly; posterior portion of the metacone is compressed; the widest point of the metacone is more anterior; and the width of the lingual cusps is greater. While these differences are visible in the thin plate spline, they are also more clear in relationship to the actual tooth in the averaged (consensus) image (Figure 8).

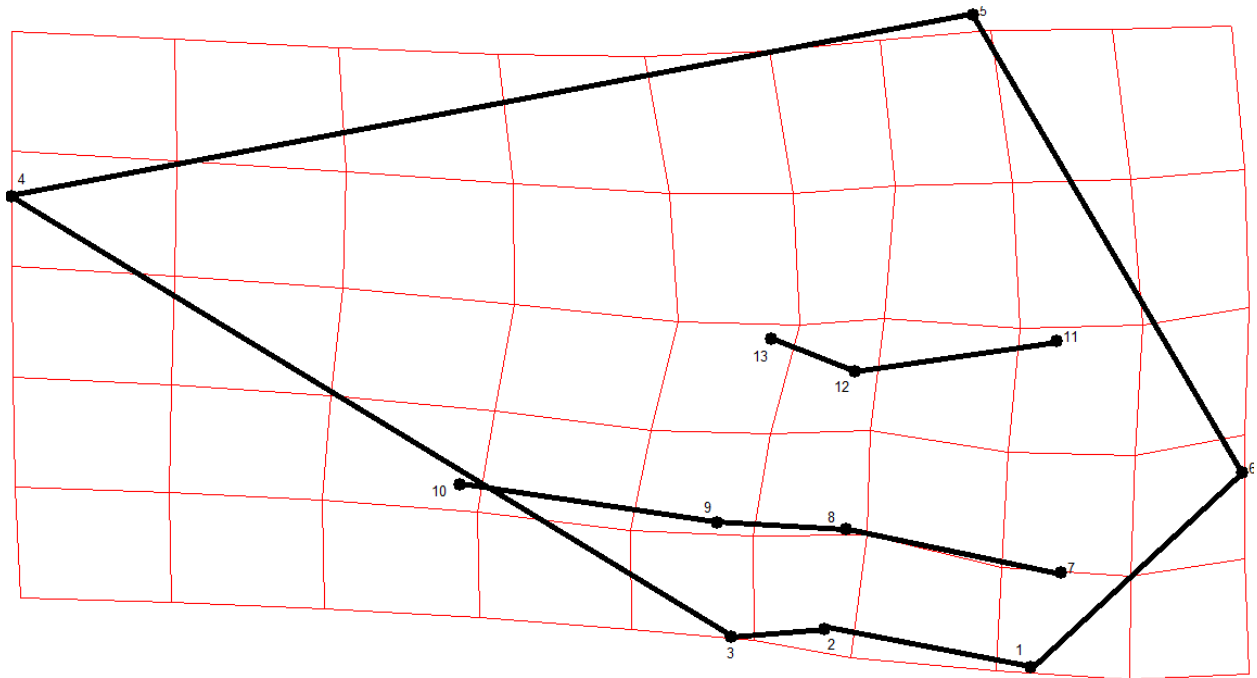


Figure 7. Thin Plate Spline. This shows the differences in morphology when U. americanus is stretched to fit to the form of U. arctos. The outline of the tooth, labial cusps, and midline of the tooth have had their landmarks connected for the sake of recognition.



Figure 8. Averaged Images of the M2 of U. americanus (Right) and U. arctos (Left). These images help to illustrate the visual differences between the teeth, and how prominent they are between a large number of specimens.

The first major difference between the teeth of the two species of *Ursus* is that the protocone is more often split in *U. americanus*. In 27 of 37 (72.97%) specimens of *U. americanus*, the protocone is split. It is evident that the protocone is not always split, and not always split in the same location, by the lack of a clear division, but the cusps are definitely blurred between landmarks 11 and 12. While some of the same blurring is seen in *U. arctos*, it is substantially less. Only 12 of 25 (48%) of *U. arctos* specimens had a split protocone. In *U. americanus*, the labial cusps are more hexagonal, with points on the lingual side. In *U. arctos* the paracone is more strictly cuboid and the metacone is more triangular. While a presence of a post hypocone was recorded to be more common in *U. americanus*, both the hypocone and post hypocone are shown to be highly variable in size and position in both species. This region of the image shows the general shape of a cusp, but it is only very weakly and any details are very blurry. While the metaconule is also fairly blurry in both species, it is significantly more robust and distinct in *U. arctos*.

Discussion

Morphological Diagnosis

Results from the Principal Components and Discriminant analyses show a strong indication that the morphology of the M2 of *U. arctos* and *U. americanus* can be used to distinguish the two species. However, an important aspect of this study is creating a diagnostic technique that doesn't require a full statistical analysis. While the differences described in the results can be used as a general guide, the primary focus should be on the protocone, metacone, and metaconule as these are features with several landmarks

specified as important by the PCA and Discriminant analysis. As such, the criteria for identifying *U. americanus* and *U. arctos* by the M2 should go as follows: 1) if the tooth has a triangular shaped metacone and the metaconule is approximately equal in width to the metacone, then the tooth should be classified as *U. arctos*, 2) if the metacone is cuboid or hexagonal and the metaconule is visibly smaller than the metacone, then the tooth should be classified as *U. americanus*. In the case of uncertainty, secondary characteristics can be used to improve the diagnosis. While these secondary characters do appear to be indicative of species, they were variable enough that landmarks could not be regularly placed in locations associated with them. In *U. americanus*, the protocone is typically split and both the hypocone and a post-hypocone can usually be identified. The protocone is only rarely split in *U. arctos* and a post-hypocone is typically small to the point of being unidentifiable. With these traits, M2 from either modern or Pleistocene *U. americanus* and *U. arctos* can be classified to at least a conferred species designation, if not confidently to species.

Further Implications

An unexpected result from the PCA analysis of specimens from both collections was the separation of the ETVP and NMNH *U. arctos* specimens. Most of the ETVP specimens were Kodiak (*U. arctos middendorffi*), so this may be an indication of a difference in the morphology of the M2 between the continental brown bear (sampled at NMNH) and the Kodiak subspecies (ETVP sample). It appears that the *U. arctos middendorffi* lingual cusps are more blade like, making their divisions less distinct. Future studies should be conducted to see if the separation seen in the PCA and visual

difference is indicative of a true characteristic, or a trend within the species. The visual difference might not be consistent enough to be considered as a diagnostic tool, and the separation in the PCA might be due to a slight difference in the angle the photograph was taken. If a future study does show a true difference in these M2, then that might show that the technique is useful amongst a wide variety of *Ursus* species and subspecies. Distinguishing *U. americanus* from *U. thibetanus* can be difficult at times, and would likely be further complicated in the fossil record as one approaches their most recent common ancestor (Larivière 2001). Careful analysis of the M2 may be useful in distinguishing the two species. In addition, genetic studies show that other extant species of bear may also be closely related to *U. americanus*, presenting another possible candidate for analysis (Kutschera et al. 2014). While this technique has not been vetted against ursids outside of *Ursus*, it seems likely that it would be similarly effective.

Further analysis of the morphology of the M2 could reveal more than just evolutionary relationships. As the teeth are primarily used for food acquisition and processing, differences in morphology may be reflective of diet. While *U. americanus* and *U. arctos* are largely omnivorous, there are extant bears adapted for hypercarnivory, hypocarnivory, insectivory, and herbivory of hard plants (Baryshnikov 2007). Using the characters of the M2 of these different, specialized species could assist in revealing the diet of extinct bears, such as *Arctodus simus* and *Arctotherium*, whose diet is debated (e.g., Matheus 1995, Sorkin 2006, Figueirido et al. 2010, Meloro 2011). A comprehensive study of the morphology of the teeth of various fossil and

extant bear species that gives attention to functional morphology may be useful in showing why *Arctodus* and other extinct bears may have different morphologies.

While learning more about the morphology of the M2 could be useful in distinguishing other species of ursids and learning more about the diets of extinct ursids, the results of this study can directly be used for future work without secondary research. With a new method for diagnosing Pleistocene ursines from North America, specimens from locales which were difficult to diagnose can be reexamined to more strongly confirm their designation, or correct it. Genetic studies suggest that there may be specimens which are incorrectly labeled, or there is an important clade of *U. arctos* which is relatively absent from the fossil record (Davison et al. 2011). Davison et al. (2011) found that there should be a clade known as Clade 4 of *U. arctos* which migrated south of Beringia into Canada as early as 33,000 cal years BP. Very few fossils of *U. arctos* have been reliably identified and dated to older than 12,000 cal years BP (Matheus 2004). This study could be crucial in identifying any members of this clade which have been misidentified. A potential similar situation can be seen in the Meachen et al. (2016) study in which they suggested several wolves from Natural Trap Cave were misidentified and actually represented the Beringian morphotype. Both the Beringian wolf case and the Clade 4 of *U. arctos*, feature a group of animals moving south of Beringia that have not previously been identified in the fossil record.

CHAPTER 3

ECOLOGICAL NICHE MODEL OF *U. AMERICANUS* AND *U. ARCTOS* PROJECTED TO THE LAST GLACIAL MAXIMUM

In addition to the morphological study of the upper second molar, a small ecological niche study was performed to assist in selecting locations where the results of said study might be best used. As stated previously, there is potential for an overlap in *U. arctos* and *U. americanus* populations south of the Cordellian and Laurentide ice sheets as early as 31,000 cal years BP (Davison et al. 2011). The contiguous United States is quite a range of land in which to search for misidentified fossils, so a method for narrowing the search radius would be greatly beneficial. This would allow focused searching for areas where both species are predicted to have occurred, or see where a species has been identified outside of its expected range. While some areas are known to not contain *U. arctos* currently, such as eastern North America (Feldhamer et al. 2009), there are fossil specimens from the Pleistocene that have been identified as *U. arctos* as far east as Maine (Graham and Lundelius 2010). As such, it is important to not disregard that the Pleistocene was a very different time both climatically and ecologically and modern preconceptions of where these species should not be used.

For an ecological niche study, bioclimatic variables are required. While bioclimatic variables are readily available from much of recent history, there aren't any that span the entirety of the Pleistocene. However, climatic data for the Last Glacial Maximum (LGM) has been created and is available through WorldClim. The LGM, as the period with the most glaciation out of the 31,000 years that *U. arctos* could have

been present south of Beringia, acts as a good extreme for comparison with the modern climate. Something worth noting though, is that while this LGM bioclimatic data is incredibly useful, it cannot be perfectly accurate. Davis et al. (2014) suggest that ecological niche model projections of the LGM may have some strong biases. This data has been generated from a series of paleoenvironmental studies, not collected from weather stations across the world. As such, it should be subject to scrutiny, and will not be wholly accurate.

Materials and Methods

Location data for both *U. americanus* and *U. arctos* were obtained from the Global Biodiversity Information Facility (GBIF). Environmental data, in the form of bioclimatic variables, was obtained from WorldClim, this included both modern data and data from the LGM. All data processing was performed in Microsoft Office Excel and ESRI ArcGis. For several specific tasks, the SDMtoolbox add-on for ArcGis, developed by Jason L. Brown, was used.

Bioclimatic variables were chosen for this study were 1, 4, 12, and 15 which correspond to Annual Mean Temperature, Temperature Seasonality, Annual Precipitation, and Precipitation Seasonality, respectively. Only a limited number of the total possible bioclimatic variables were chosen to avoid the possibility of overfitting. These particular variables were chosen to represent the general environmental conditions at the time. Bioclimatic data was downloaded at 5 arc-minutes in ESRI Grid and CCSM4 types. ESRI Grids were used in the modern model and CCSM4 in the LGM model. All bioclimatic variables were masked to North America. Species data from GBIF

was rarefied to 8 km and masked to North America. Eurasian *U. arctos* were considered for inclusion, but ultimately excluded. This was done to avoid any complications caused by differences in environmental preferences between the North American and Eurasian clades. While North American clades are descended from Eurasian clades, genetic studies have shown that there is not any significant level of interbreeding with Eurasian clades once *U. arctos* actually extends into North America. Once rarefied and masked, species data was divided into 80% training and 20% testing subsets.

Both ecological niche models were performed using Maxent. As Maxent is a relatively easy to use, common, and stable modeling package, it was the software of choice. Maxent models were ran using 10 percentile training presence as the threshold rule. Young et al. suggests that this threshold rule is suitable for testing subsets greater than 10%. Maxent first generated an ecological niche model for the present distribution of both *U. arctos* and *U. americanus*. From the data of the present ecological niche model, the LGM model could be created using the LGM bioclimatic variables. Rasters from the four niche models were converted to binary at a .5 threshold. At this threshold, a presence estimate of less than 50% would be considered absence and an estimate of greater than 50% would be considered presence. While this does simplify the map, it allows for comparison between modern and LGM models and helps to counter overfitting of the model. Presence maps that have not been simplified to binary are still important, as they show a total range, and are useful in the case that the binary map under-fits the total range. Once converted to binary, the LGM projection rasters were reclassified to 1 and 4 as opposed to the 0 and 1 of binary for raster addition and

subtractions. Modern model rasters were subtracted from the LGM model rasters to allow for visual representation of the differences.

Results

The ecological niche models for the modern (Figures 9 and 20) and LGM (Figures 10 and 11) distributions of both *U. americanus* and *U. arctos* can be seen in the figures below. Accuracy metrics suggest a strong, though imperfect level of accuracy. Both area under the curve (AUC) values for the Sensitivity versus Specificity charts (Figure 12) generated by Maxent scored above 8.5, with the Ecological Niche Model for *U. arctos* scoring at slightly higher.

The modern ecological niche model for *U. americanus* (Figure 9) shows the strongest presence along the west coast, followed by the Rocky Mountains and east coast with a preference for the upper east coast. The only areas of strong absence are the northern most portion of Canada and Alaska, the Yucatan Peninsula, and the Sonoran and Mojave Deserts. For *U. arctos*, the modern ecological niche model shows the strongest presence along the Canadian and Alaskan west coast and the Rocky Mountains. Areas of moderate to light presence include the Chihuahua Mountains in Mexico and most of Canada reaching to the east coast. Areas of absence include the Arctic, the middle and eastern areas of the United States, and portions of Mexico and the western United States.

Potential Presence of *U. americanus*: Modern

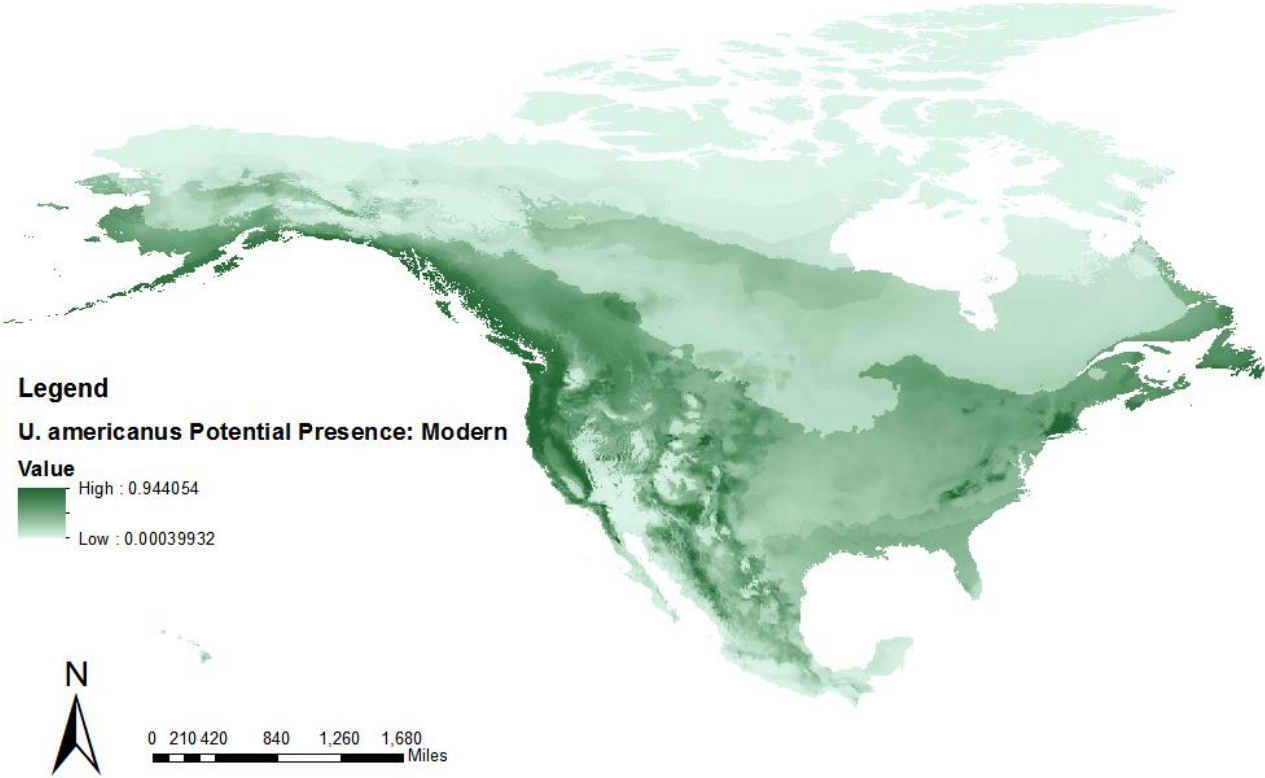


Figure 9. Modern Ecological Niche Model for *U. americanus*.

Potential Presence of *U. arctos*: Modern

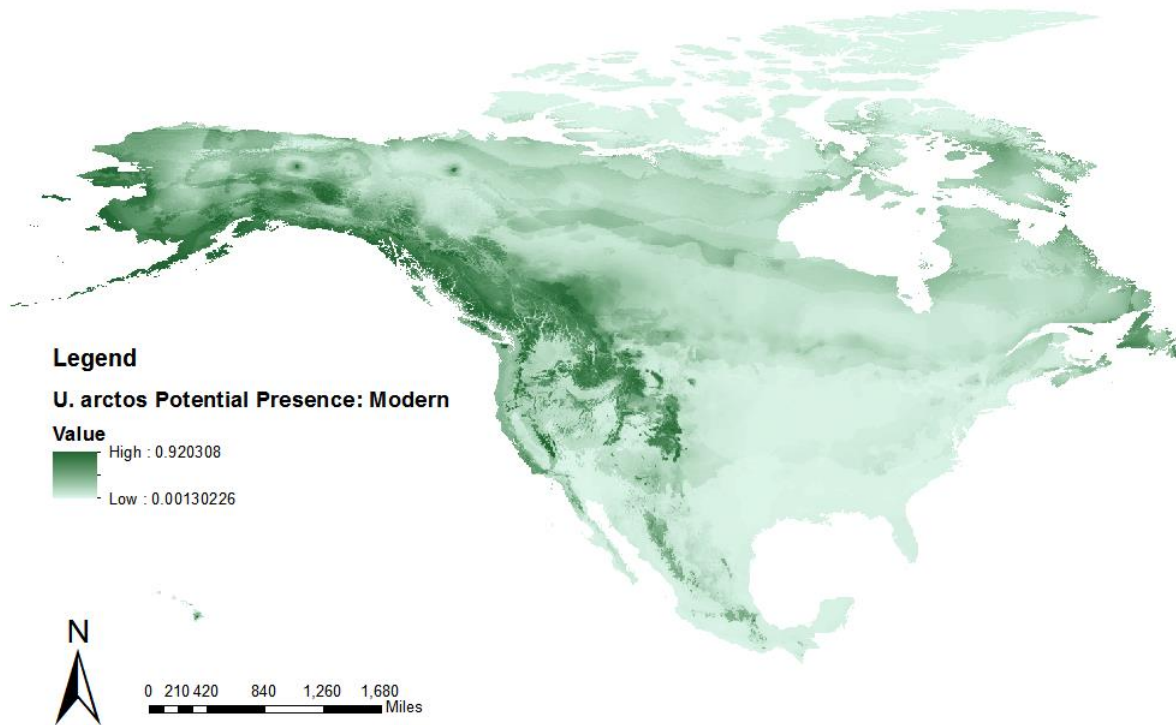


Figure 10. Modern Ecological Niche Model for U. arctos. Note that this model is restricted to North America, so it does not take the Eurasian range into account.

U. americanus Potential Presence: LGM

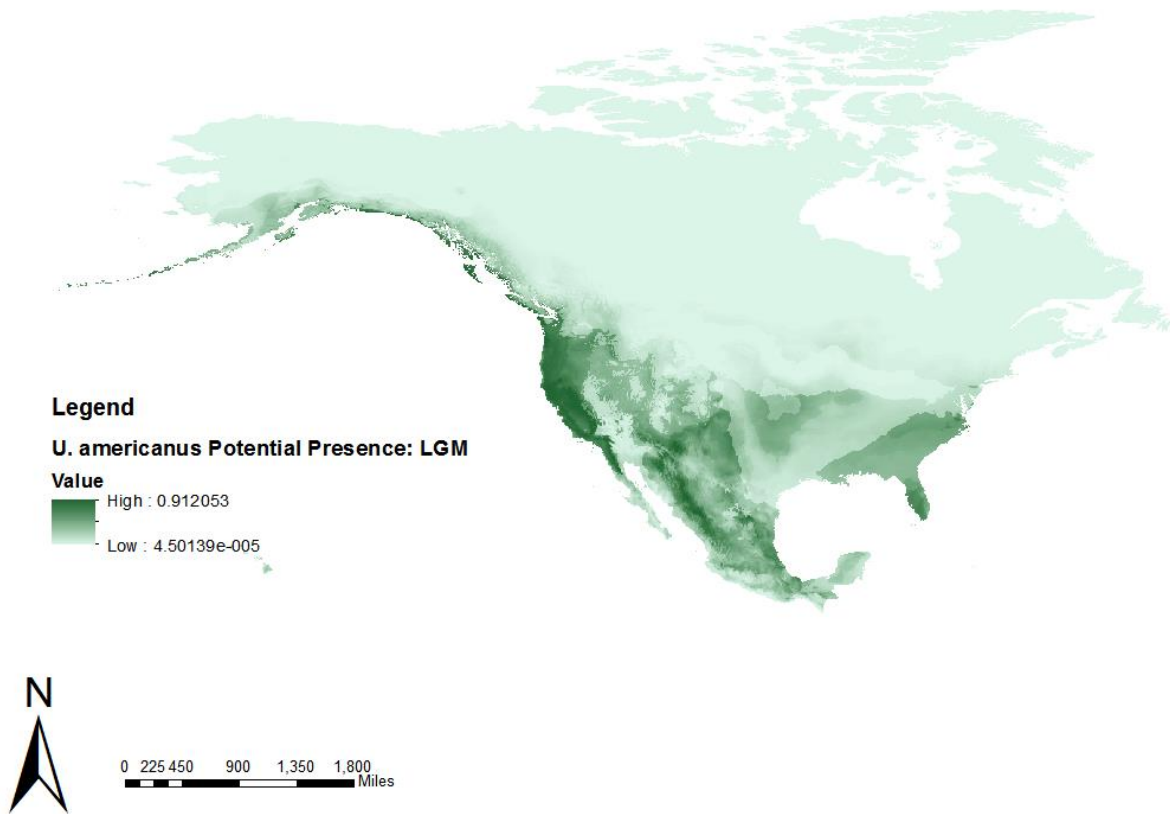


Figure 11. Last Glacial Maximum Ecological Niche Model for U. americanus. This model represents the range of U. americanus at approximately 21,000 years cal BP.

Potential Presence of *U. arctos*: LGM

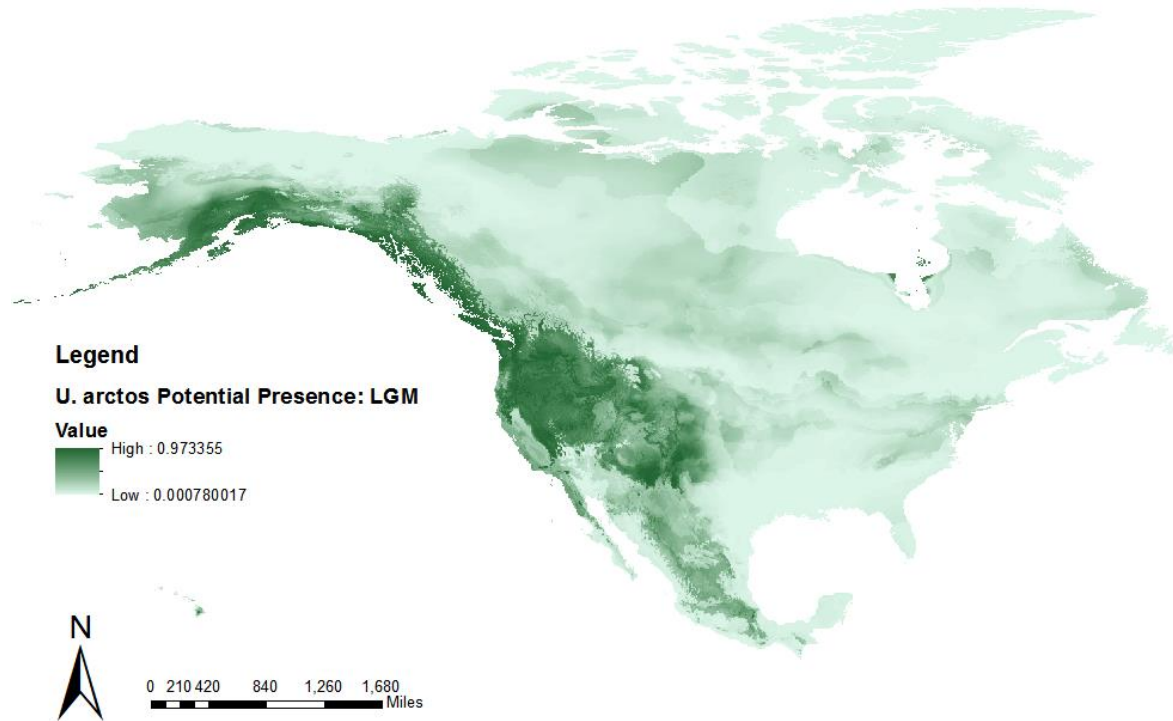


Figure 12. Last Glacial Maximum Ecological Niche Model for U. arctos. This model represents the range of U. americanus at approximately 21,000 years cal BP.

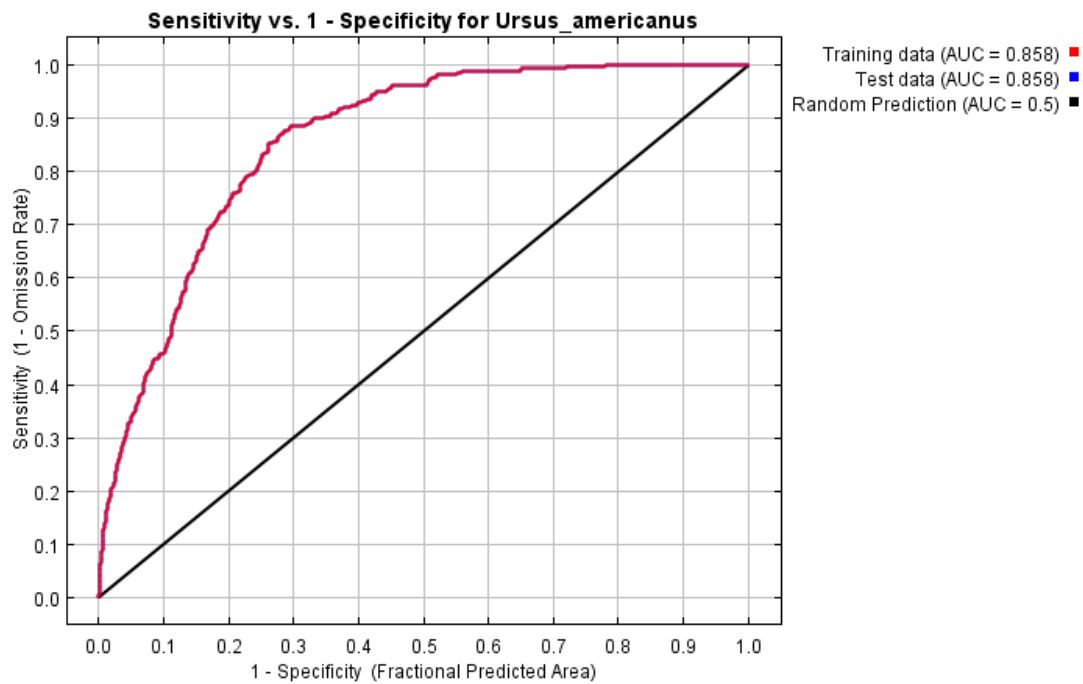
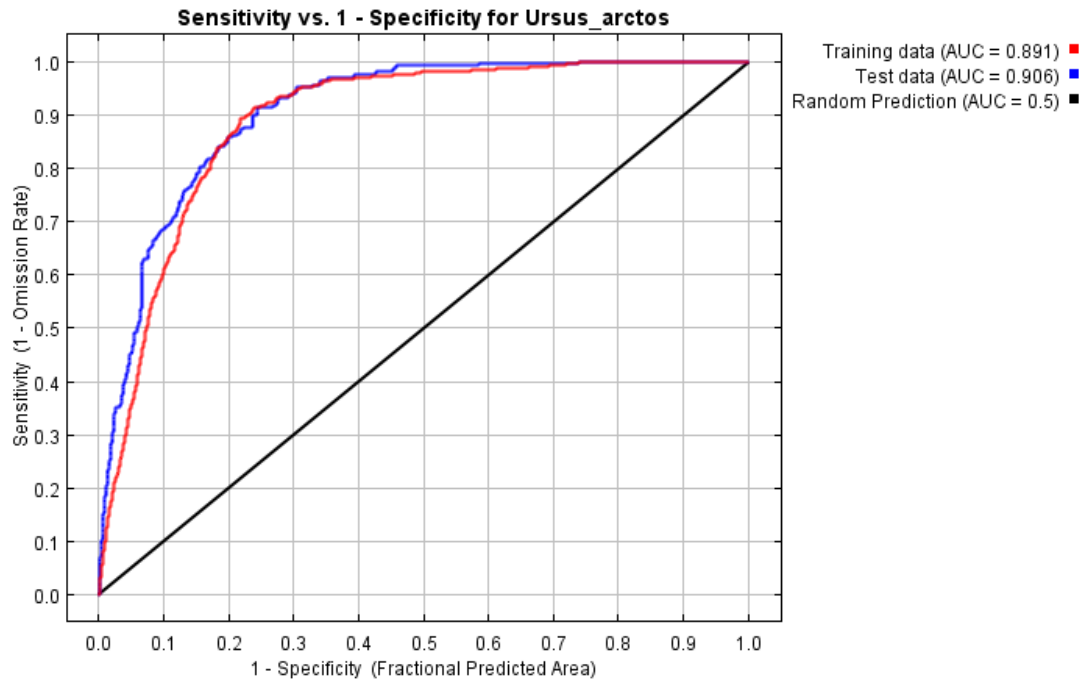


Figure 13. Sensitivity vs. Specificity charts for the Ecological Niche Models. A value of .5 is equivalent to random chance, with a value of 1 being absolute certainty.

The LGM ecological niche model for *U. americanus* shows strong presence along the west coast, narrowing to the coast line along the northern portions, the Chihuahua Mountains, the east of the United States, and portions of most of the midcontinent. *Ursus americanus* does show absence across nearly the entirety of Canada aside from portions of the south and a narrow strip of the west coast. This is likely due to the presence of the Cordilleran and Laurentide ice sheets spread across Canada. The LGM ecological niche model for *U. arctos* shows very strong presence along the Canadian and Alaskan west coast, most of the United States west coast, and much of the western half of the United States. There is strong, though lighter presence throughout much of Mexico, and light presence spreading throughout much of the continent, all the way to the east coast.

When converted to a binary map, and compared to the modern distribution (Figures 14, 15, and 16), *U. americanus* is shown by the ecological niche model to have a greater range along the west coast and southern range, but reduced presence in the north. In *U. arctos*, the ecological niche model shows a much greater area of presence along the west coast and western half of the United States. This said, there is less presence along the north-western coast of Alaska and parts of Canada. There are three principal areas of overlap for the two species in the LGM ecological niche model: A large portion of the western corner of the United States, a narrow strip along the Canadian west coast, and a portion of the central United States.

Changes to *U. americanus* Distribution

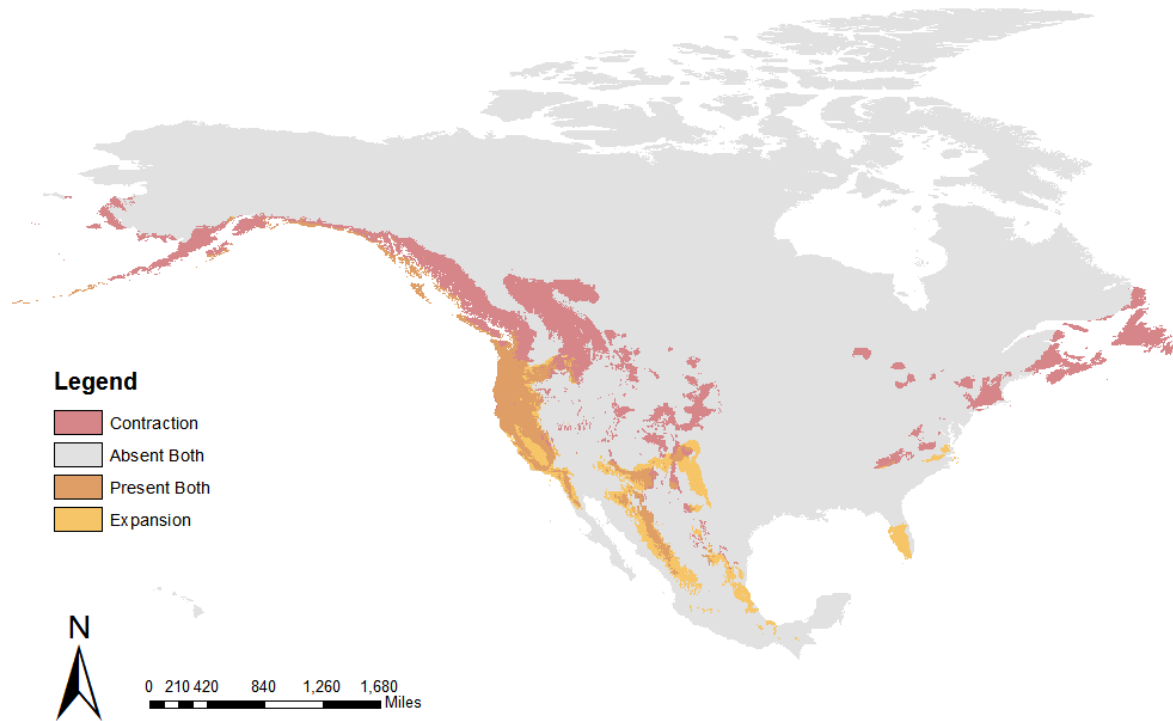


Figure 14. Comparison of the U. americanus Modern and LGM Ecological Niche Model. Areas of high presence (>.5) of U. americanus compared between the current to LGM model.

Changes to *U. arctos* Distribution

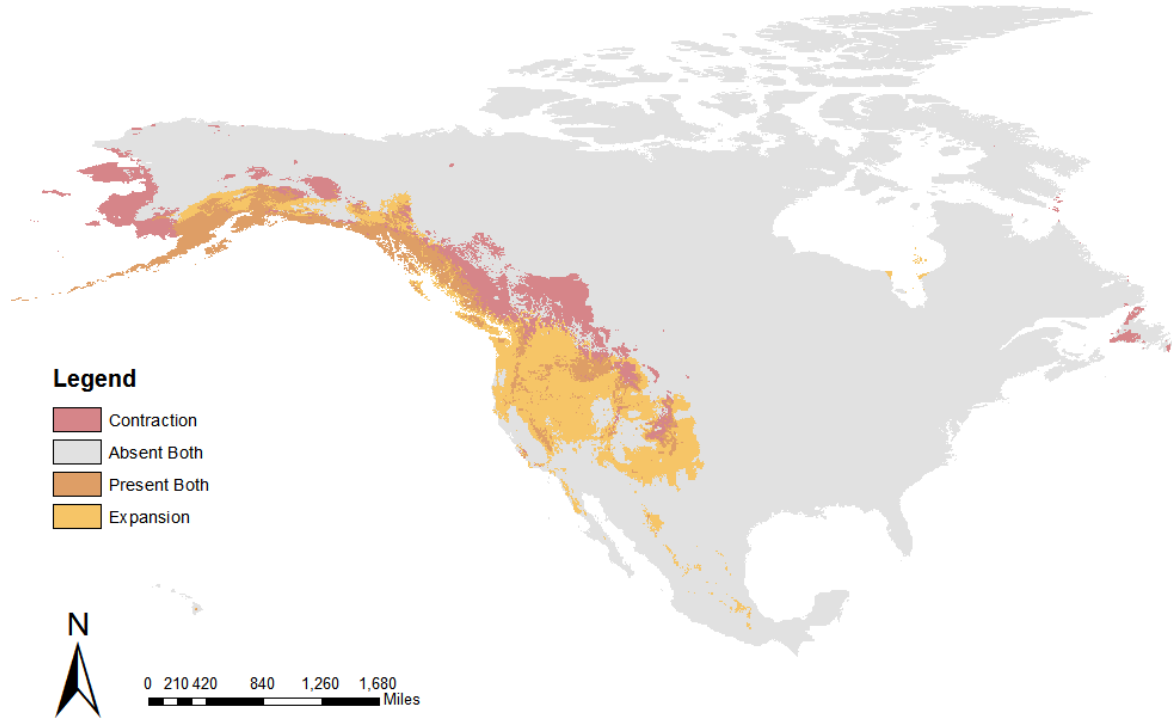


Figure 15. Comparison of the U. arctos Modern and LGM Ecological Niche Model.

Areas of high presence (>.5) of U. arctos compared between the current to LGM model.

Overlap of *U. arctos* and *U. americanus* at LGM

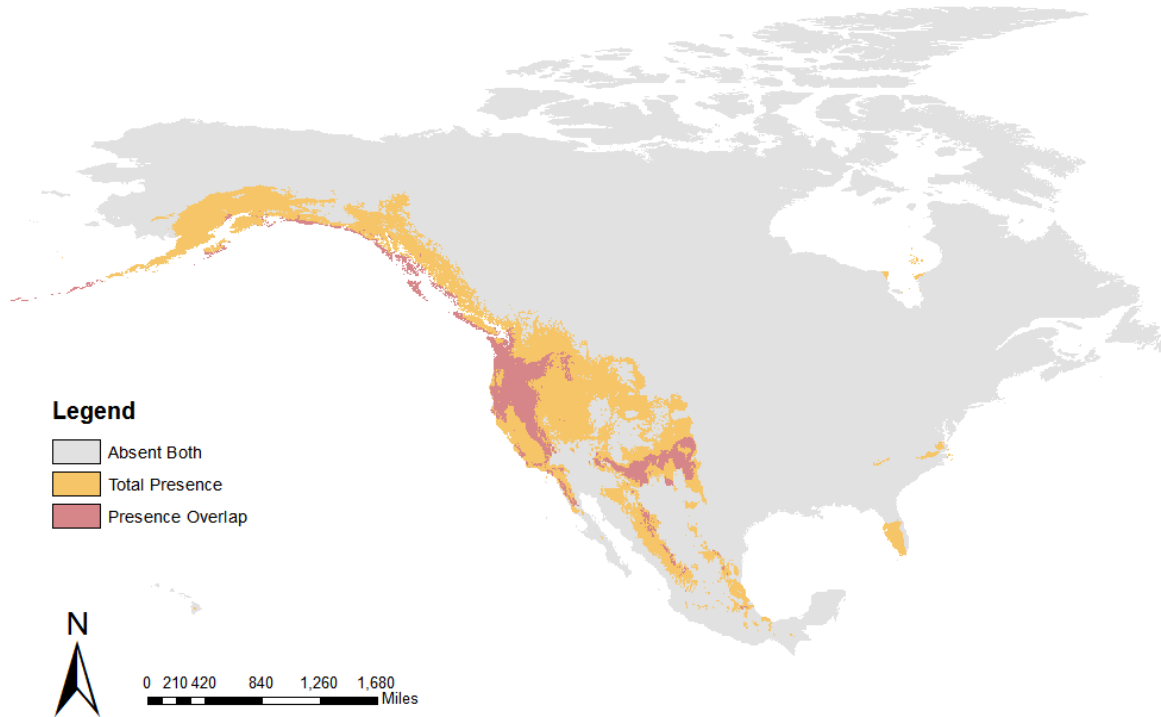


Figure 16. Area of significant presence (>.5) overlap between U. americanus and U. arctos at the LGM (~21,000 cal years BP).

Discussion

The ecological niche models have a strong level of accuracy based upon their AUC scores, and a comparison with the modern historic range of both species shows a strong similarity. The *U. americanus* historic range (Pelton et al. 1999) matches the niche model closely, and while the *U. arctos* model includes everywhere that *U. arctos* occurs, it does seem to over fit as it shows light presence along the east coast (Feldhamer et al. 2003). This said, the LGM niche model, as well as several fossil localities suggest that *U. arctos* used to inhabit this area (Graham and Lundelius 2010). This suggests that the model may not actually be overfitting, but simply cannot account for some other environmental factor. A difference in available food or vegetation between the LGM and present could be the cause of this range reduction. While a vegetation index can be included in modern ecological niche models, they have not been created for the LGM. Niche models could be created to account for the presence or absence of the food items for *U. arctos*, but as *U. arctos* can consume a very wide variety of food items, the scale of that task puts it outside the scope of this study.

The large area of strong presence for *U. arctos* south of Beringia in the LGM ecological niche model suggests that *U. arctos* would have been successful throughout much of North America. The presence of *U. arctos* fossils as far east as Maine suggest that the light presence in that area may have been stronger than indicated, or at least stronger at a later point in the Pleistocene (Graham and Lundelius 2010).

With a particularly low presence in the southeast of the United States from *U. arctos*, and the opposite with *U. americanus*, this may be the only area south of the ice sheets where the two species did not coexist, or were unlikely to do so. In all other

areas south of the ice sheet, both species have potential presence, but at varying degrees. As such, identifications should not be made based on location. This is especially important in the areas of strong overlap, namely the west coast and Rocky Mountains. These are areas where a careful identification is especially important, as both species could easily be present. The other two areas of concern are the southeast and the majority of Canada. These are areas where one species is present, and the other is largely absent. Specimens found in these areas that have been identified as a species other than that expected by the ecological niche model should be closely analyzed based upon the morphological study shown previously. This said, it is possible that the ecological niche model is not accurately representing these areas, or that the specimen has wandered from its typical range, so these specimens should not be identified based solely on their location.

CHAPTER 4

CASE STUDY AND CONCLUSIONS

Through a morphometric analysis of the second upper molar, this study has strived to develop an improved technique for the identification of *Ursus* species in North America. In addition, niche models were developed to help identify areas where each fossil species was likely to occur during the LGM. While the morphological analysis and the ecological niche models can be used independently, they can also be used in conjunction to assess the record of LGM bears across North America. The niche models can be used to identify fossil sites where one or both species of *Ursus* would be expected to occur, and the morphological analyses can be used to assist in the identification of any specimens found at those localities. Additionally, this pair of studies can be used in conjunction with FAUNMAP to check for localities that report a specimen outside of its expected range or report one expected species but not the other.

While this study appears successful in generating a technique for identifying specimens and locating where they are likely to occur, this success is based on AUC values and degrees of separation. The real degree of success is to be seen in the successful application of these techniques. FAUNMAP lists six specimens of *U. arctos* in the eastern half of North America that date to the Pleistocene. While the ecological niche model for the LGM shows that there was some presence of *U. arctos* in this area, the presence is at a very low number, so fossils from this area might be uncommon.

Two Pleistocene specimens previously identified as *Ursus arctos* from the Carnegie Museum of Natural History were borrowed for analysis. This includes CM 12617, from Welsh Cave, KY, and CM 12999 from Organ Cave, WV. Both specimens

are reported in the literature as *U. arctos* (Guilday 1968, Guilday et al. 1977). Guilday (1968) and Guilday et al. (1977) do not state how these two specimens are identified, but as CM 12617 is 34mm long and CM 12999 is 33mm long, it seems that if Kurtén and Anderson's (1980) method of identification by tooth length was considered, it would not have been particularly useful. Kurtén and Anderson (1980) stated, and Graham (1991) restated, that the M2 of fossil *U. americanus* never exceeded 34mm in length, and that fossil *U. arctos* rarely had M2 of such a short length. At 33mm and 34 mm in length, the M2s of these two specimens would be difficult to identify by tooth length. Hence, these two specimens were a prime candidate for a case study attempting to support their identification, or re-identify them.

The method for visually identifying the two species described on page 33, was applied to both teeth, with mixed results. Images of these teeth can be found in Appendix A. CM 12617 was determined to be correctly identified based on the presence of a large metaconule and triangular metacone. CM 12999 was determined to be incorrectly identified based on a relatively small metaconule, and cuboid metacone. It should be noted that CM 12999 is unusual in that it appears to have an accessory cusp sitting posterior to the metacone, potentially compacting it. While this accessory cusp could be masking a more triangular shape for the metacone, the small size of the metaconule suggests that this is not the case. As such this study refers CM 12999 to *U. americanus*.

In order to strengthen this referral, as this would be the first application of this technique to a fossil specimen, photographs of CM 12617 and 12999 were landmarked

and included in a principal component analysis and discriminant analysis alongside the specimens from the NMNH and ETVP collections.

The principal component analysis shows very similar eigenvalues and principal components to the previous principal component analysis (Tables 6 and 7). The two scatterplots (Figures 17 and 18) show that the fossil specimens plot within the morpho space of their expected identifications, though they are not nestled closely within that morpho space.

The discriminant function and stepwise discriminant function show eigenvalues and Wilk's lambdas very similar to the previous discriminant functions (Tables 8 and 9). However, the discriminant function did not misidentify as many specimens as *U. arctos*, increasing its success rate somewhat (See Appendix A). Additionally, the fossil specimens are classified as their expected groups, with CM 12617 classified as *U. arctos* and CM 12999 classified as *U. americanus* (Figures 19 and 20).

The results of the principal component analysis and discriminant functions indicate that these two fossil specimens do not share the same species morpho space and are classified differently statistically. This difference in principal component and discriminant function scores agrees with the results of the morphological diagnosis, so this study would redesignate CM 12999 as *U. americanus*. This case study serves as an example of how this type of study is useful, and exemplifies the difficulty of identification without it. In the future, this analysis can be used to facilitate the identifications of *Ursus* specimens across North America, and potentially uncover previously under represented clades within *U. arctos* that have been misidentified.

Table 6. Total Variance Explained for the Case Study Principal Component Analysis.

Total Variance Explained

Component	Initial Eigenvalues			Extraction Sums of Squared Loadings		
	Total	% of Variance	Cumulative %	Total	% of Variance	Cumulative %
1	7.004	26.937	26.937	7.004	26.937	26.937
2	3.491	13.427	40.365	3.491	13.427	40.365
3	2.623	10.089	50.454	2.623	10.089	50.454
4	2.087	8.027	58.481	2.087	8.027	58.481
5	1.866	7.177	65.657	1.866	7.177	65.657
6	1.476	5.678	71.336	1.476	5.678	71.336
7	1.328	5.109	76.445	1.328	5.109	76.445
8	1.047	4.029	80.474	1.047	4.029	80.474
9	.939	3.612	84.086			
10	.620	2.383	86.469			
11	.579	2.229	88.698			
12	.526	2.023	90.720			
13	.462	1.776	92.496			
14	.399	1.534	94.030			
15	.356	1.370	95.400			
16	.284	1.094	96.494			
17	.262	1.009	97.503			
18	.207	.795	98.299			
19	.165	.634	98.933			
20	.127	.489	99.422			
21	.091	.350	99.772			
22	.059	.227	99.999			
23	.000	.000	99.999			
24	9.928E-5	.000	100.000			
25	6.583E-5	.000	100.000			
26	3.106E-5	.000	100.000			

Extraction Method: Principal Component Analysis.

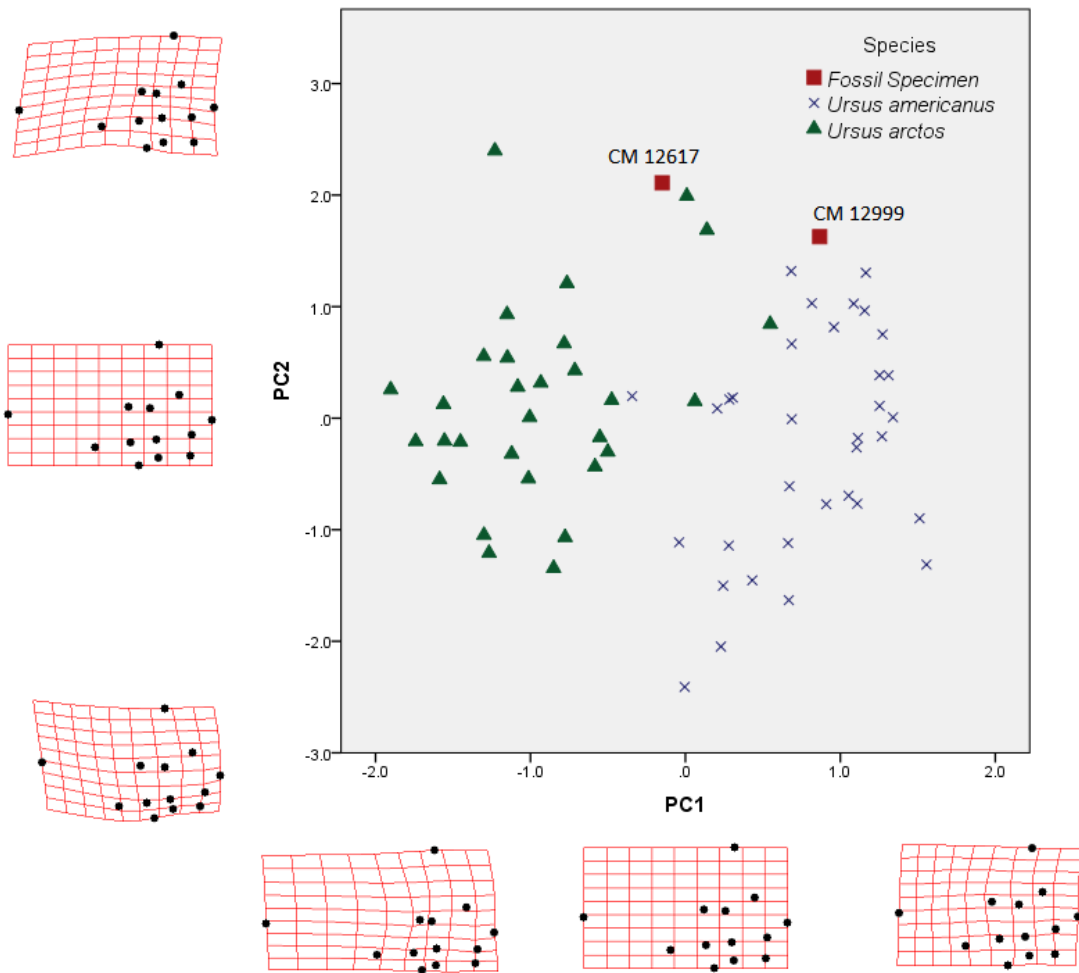


Figure 17. Scatter Plot of the Case Study PC1 and PC2. The first principal component shows lateral compression or extension with an inverse effect along the anterior landmarks. The second principal component shows a vertical bending of the anterior landmarks of the tooth.

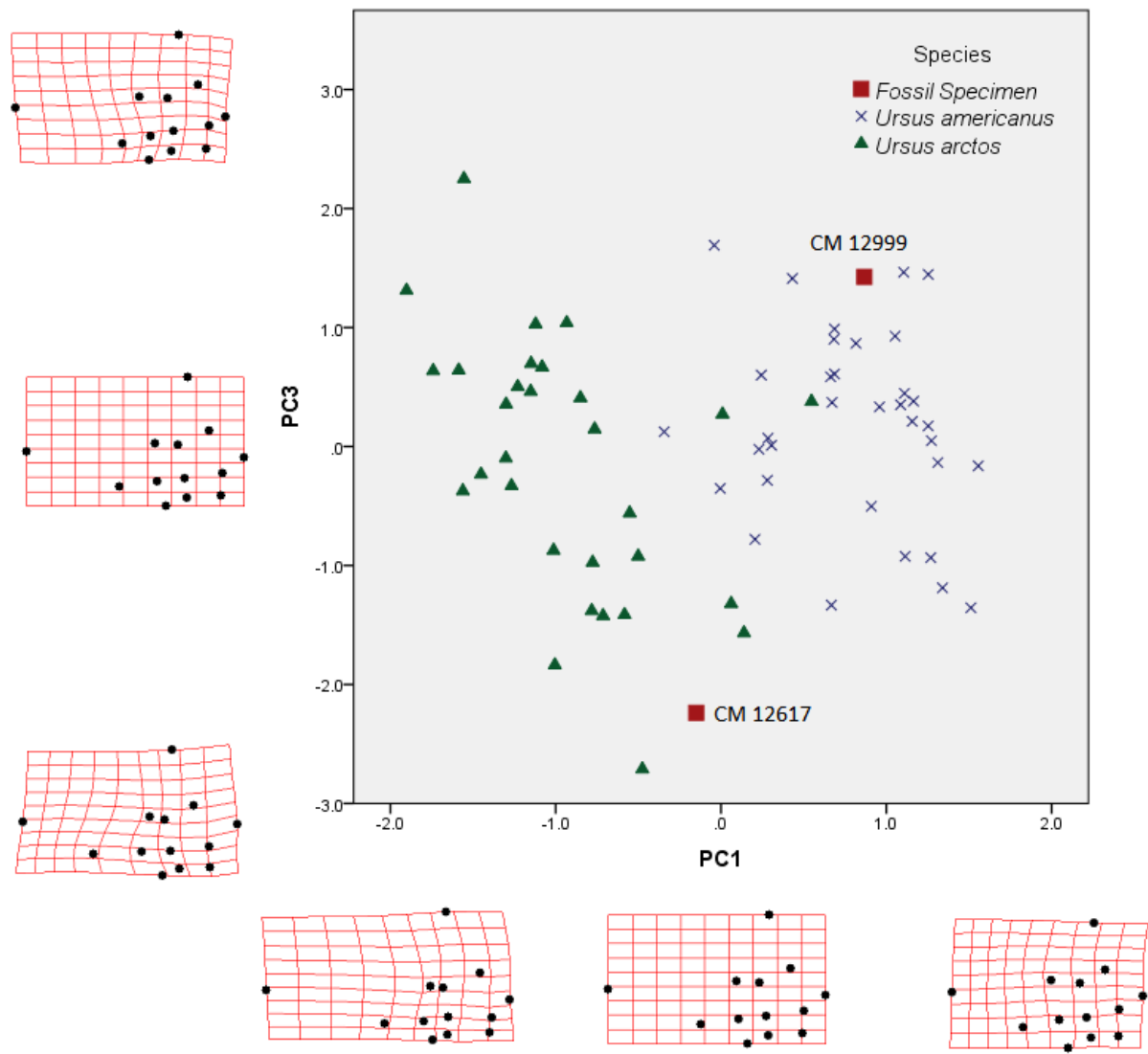


Figure 4. Scatter Plot of the Case Study PC1 and PC3. The first principal component shows lateral compression or extension with an inverse effect along the anterior landmarks. The third principal component shows a twisting such that the lingual and labial sides of the middle of the tooth inversely compress or expand.

Table 7. Component Matrix for the Case Study Principal Component Analysis

Component Matrix^a

	Component							
	1	2	3	4	5	6	7	8
X1	-.207	-.077	-.119	-.766	-.189	-.024	.208	-.009
X2	.458	-.205	-.421	-.007	.324	.273	.366	.163
X3	-.447	.076	-.600	.160	.373	-.119	.203	.002
X4	.823	-.358	-.277	-.002	-.241	.058	-.093	-.006
X5	.495	.504	.198	-.320	.283	-.244	.203	.021
X6	.462	-.099	-.529	.159	-.380	.020	-.102	-.220
X7	-.132	-.353	.096	.194	-.311	.567	-.031	-.437
X8	.157	.177	.309	.612	.212	.371	.150	.039
X9	-.377	.206	.416	.291	.419	.086	-.105	-.252
X10	-.350	-.129	.650	.000	.128	-.296	-.063	-.175
X11	-.341	-.251	.260	-.313	-.210	.172	-.624	.254
X12	.098	.011	.258	.406	-.250	.255	.116	.710
X13	-.696	.343	-.276	.182	-.108	-.215	-.009	.121
Y1	-.668	-.432	.075	-.219	.199	.099	.360	.074
Y2	-.812	-.204	.116	-.090	-.250	-.035	.212	.116
Y3	-.894	.030	.058	.000	-.207	-.089	.049	-.004
Y4	-.293	-.798	-.002	.008	.288	.192	.030	-.104
Y5	.042	-.405	-.075	.498	-.132	-.580	-.193	.100
Y6	.338	-.244	-.379	-.171	.483	.045	-.492	.125
Y7	.597	.368	.218	-.345	.291	.213	-.169	.112
Y8	-.281	.765	.153	-.041	-.006	.228	-.161	-.058
Y9	.011	.681	-.159	-.126	-.488	.160	.118	-.064
Y10	-.298	.552	-.568	.236	.104	.071	-.151	-.059
Y11	.772	-.237	.192	-.023	-.172	-.032	.198	-.082
Y12	.757	.122	.275	.165	-.058	-.320	.086	-.128
Y13	.837	-.006	.250	.003	-.086	-.051	.119	.028

Extraction Method: Principal Component Analysis.

a. 8 components extracted.

Table 8. Eigenvalues (Top), Wilk's Lambda (Middle), and Classification Results (Bottom) of the Case. Classification results show a strong level of accuracy.

Eigenvalues

Function	Eigenvalue	% of Variance	Cumulative %	Canonical Correlation
1	8.686 ^a	100.0	100.0	.947

a. First 1 canonical discriminant functions were used in the analysis.

Wilks' Lambda

Test of Function(s)	Wilks' Lambda	Chi-square	df	Sig.
1	.103	115.803	22	.000

Classification Results^{a,c}

			Predicted Group Membership		Total
			1	2	
Original	Count	1	34	0	34
		2	0	30	30
		Ungrouped cases	1	1	2
	%	1	100.0	.0	100.0
		2	.0	100.0	100.0
		Ungrouped cases	50.0	50.0	100.0
Cross-validated ^b	Count	1	33	1	34
		2	2	28	30
		Ungrouped cases	33	27	60
	%	1	97.1	2.9	100.0
		2	6.7	93.3	100.0
		Ungrouped cases	55.0	45.0	100.0

a. 100.0% of original grouped cases correctly classified.

b. Cross validation is done only for those cases in the analysis. In cross validation, each case is classified by the functions derived from all cases other than that case.

c. 95.3% of cross-validated grouped cases correctly classified.

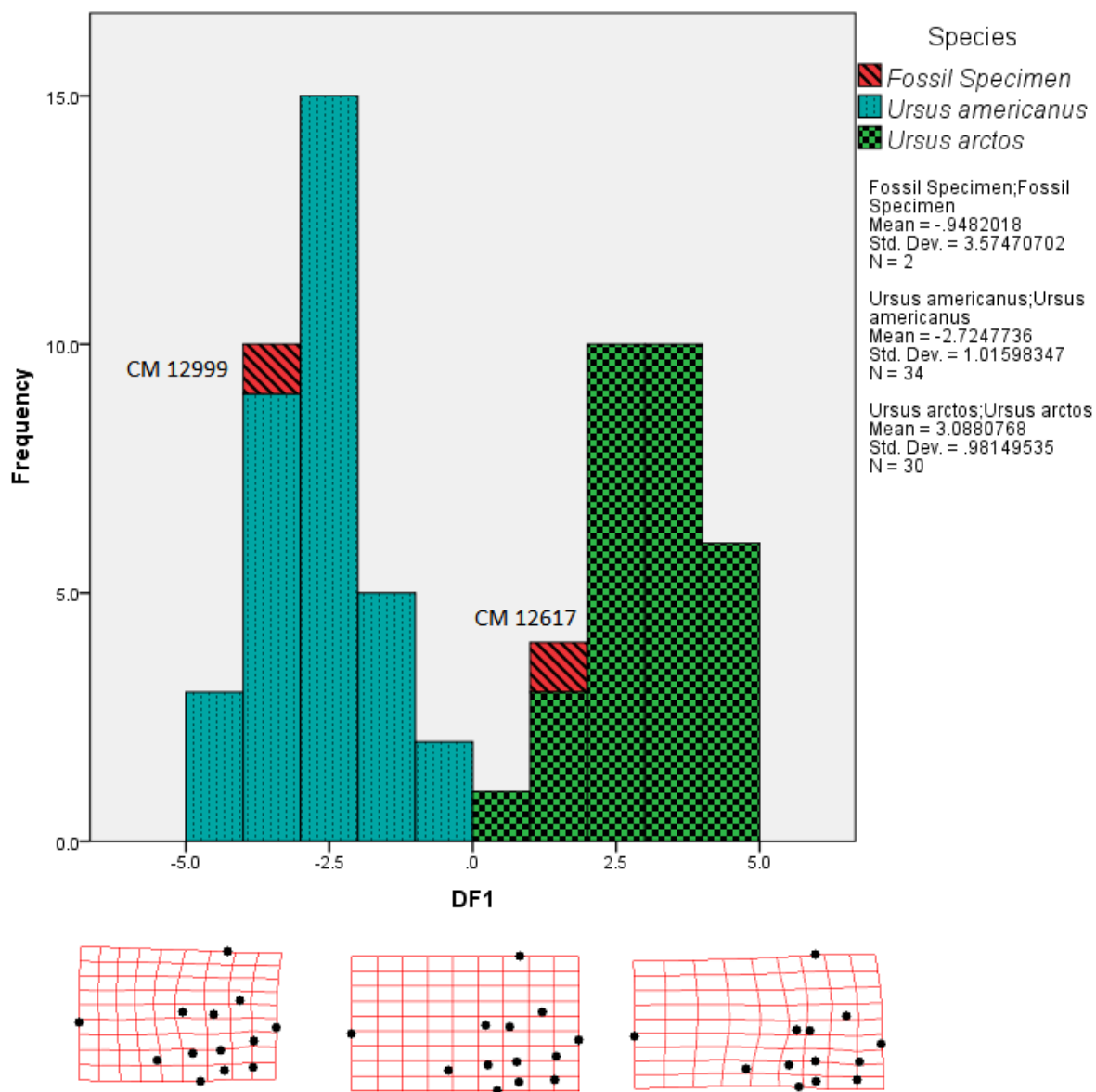


Figure 19. Histogram Plot of the Case Study Discriminant Function. The discriminant function represents the same variation as the first principal component.

Table 9. Stepwise Eigenvalues (Top), Wilk's Lambda (Middle), and Classification Results (Bottom) of the Case Study. Classification results show a strong level of accuracy, though the presence of a possibly misidentified specimen within the collection lowers the accuracy of *U. arctos* identification to 96.66%.

Eigenvalues

Function	Eigenvalue	% of Variance	Cumulative %	Canonical Correlation
1	5.041 ^a	100.0	100.0	.913

a. First 1 canonical discriminant functions were used in the analysis.

Variables Entered/Removed^{a,b,c,d}

Step	Entered	Wilks' Lambda							
		Statistic	df1	df2	df3	Exact F			
						Statistic	df1	df2	Sig.
1	Y3	.308	1	1	62.000	139.525	1	62.000	.000
2	Y10	.235	2	1	62.000	99.146	2	61.000	.000
3	Y13	.203	3	1	62.000	78.475	3	60.000	.000
4	Y8	.181	4	1	62.000	66.751	4	59.000	.000
5	X6	.166	5	1	62.000	58.475	5	58.000	.000

At each step, the variable that minimizes the overall Wilks' Lambda is entered.

- a. Maximum number of steps is 52.
- b. Minimum partial F to enter is 3.84.
- c. Maximum partial F to remove is 2.71.
- d. F level, tolerance, or VIN insufficient for further computation.

Classification Results^{a,c}

			Predicted Group Membership		Total
			1	2	
Original	Count	1	34	0	34
		2	0	30	30
		Ungrouped cases	1	1	2
	%	1	100.0	.0	100.0
		2	.0	100.0	100.0
		Ungrouped cases	50.0	50.0	100.0
Cross-validated ^b	Count	1	34	0	34
		2	0	30	30
		Ungrouped cases	1	1	2
	%	1	100.0	.0	100.0
		2	.0	100.0	100.0
		Ungrouped cases	50.0	50.0	100.0

- a. 100.0% of original grouped cases correctly classified.
- b. Cross validation is done only for those cases in the analysis. In cross validation, each case is classified by the functions derived from all cases other than that case.
- c. 100.0% of cross-validated grouped cases correctly classified.

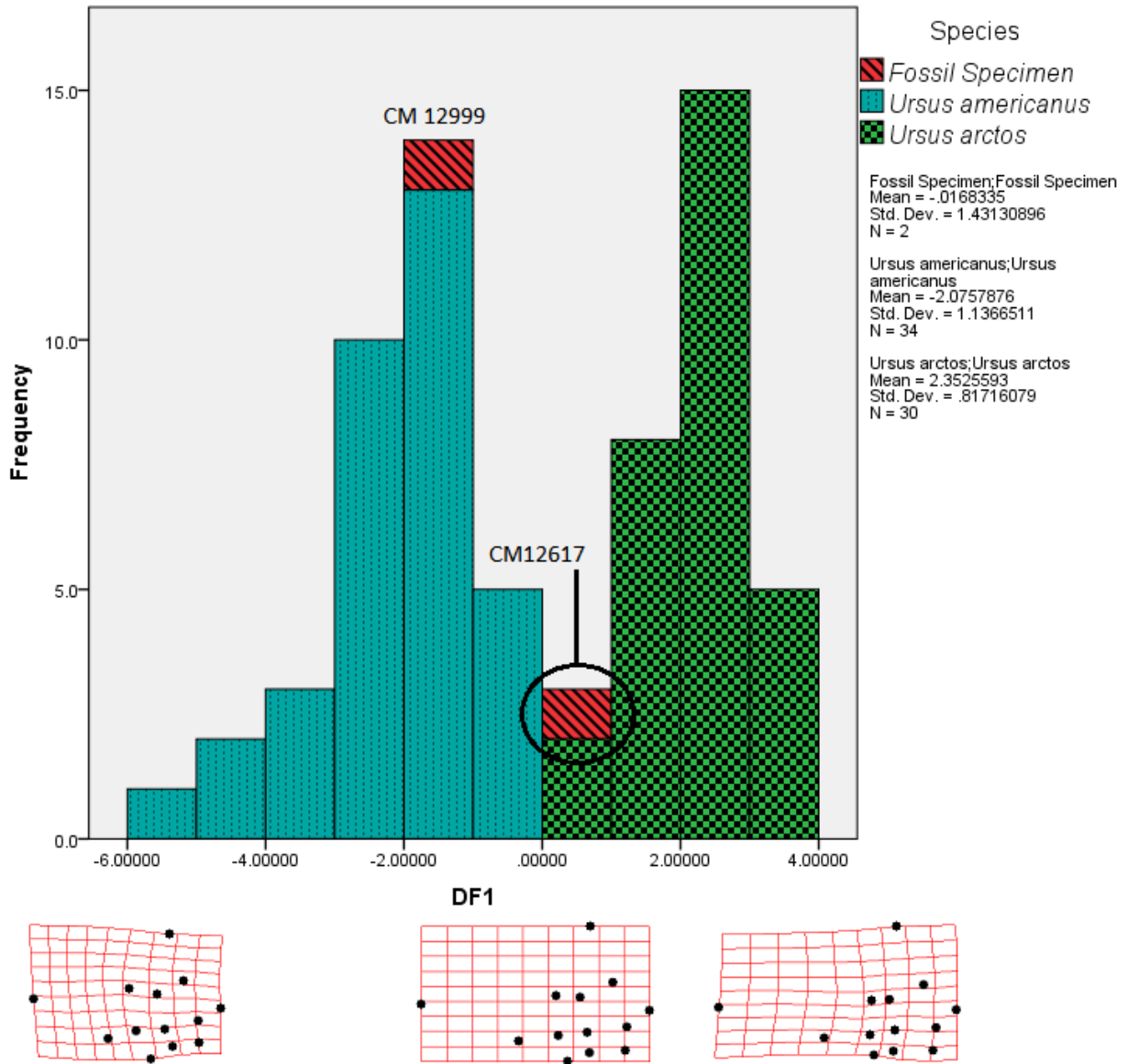


Figure 20. Histogram Plot of the Case Study Stepwise Discriminant Function. The stepwise discriminant function represents very similar variation as the discriminant function.

BIBLIOGRAPHY

- Baryshnikov, G. 2006. Morphometrical variability of cheek teeth in cave bears. *Scientific Annals, School of Geology Aristotle University of Thessaloniki (AUTH)* 98:79-102.
- Baryshnikov G, Germonpré M, Sablin M. 2003. Sexual dimorphism and morphometric variability of cheek teeth of the cave bear (*Ursus spelaeus*). *Belgian Journal of Zoology* 133(2):111-120.
- Baryshnikov, G. 2007. Bears Family (Carnivora, Ursidae). *Fauna of Russia and Neighbouring Countries* 147.
- Bookstein, F.L. 1991. *Morphometric tools for landmark data: geometry and biology*. Cambridge University Press.
- Czaplewski NJ, Puckette WL. 2015. Late Pleistocene Remains of an American black bear (*Ursus americanus*) and Two Small Vertebrates from an Oklahoma Ozark Cave 94.
- Czaplewski NJ, Willsey S. 2013. Late quaternary brown bear (Ursidae: *Ursus cf. arctos*) from a cave in the Huachuca Mountains, Arizona.
- Czaplewski NJ, Mead J, Bell CJ, Peachey WD, Ku T. 1999. Papago Springs Cave revisited, part II: vertebrate paleofauna. *Occasional Papers of the Oklahoma Museum of Natural History*.

- Davis EB, McGuire JL, Orcutt JD. 2014. Ecological niche models of mammalian glacial refugia show consistent bias. *Ecography* 37(11):1133-1138.
- Davison J, Ho SY, Bray SC, Korsten M, Tammeleht E, Hindrikson M, Østbye K, Østbye E, Lauritzen S, Austin J. 2011. Late-Quaternary biogeographic scenarios for the brown bear (*Ursus arctos*), a wild mammal model species. *Quaternary Science Reviews* 30(3):418-430.
- DeMaster DP, Stirling I. 1981. *Ursus maritimus*. *Mammalian Species* 145:1-7.
- Elftman, H.O. 1931. Pleistocene mammals of Fossil Lake, Oregon. *American Museum Novitates* 481.
- Feldhamer GA, Thompson BC, Chapman JA. 2003. *Wild mammals of North America: biology, management, and conservation*. JHU Press.
- Figueirido B, Pérez-Claros JA, Torregrosa V, Martín-Serra A, Palmqvist P. 2010. Demythologizing *Arctodus simus*, the 'short-faced' long-legged and predaceous bear that never was. *Journal of Vertebrate Paleontology* 30(1):262-275.
- Gordon, K.R. 1977. Molar measurements as a taxonomic tool in *Ursus*. *Journal of Mammalogy* 58(2):247-248
- Graham, R.W. 1991. Variability in the size of North American Quaternary black bears (*Ursus americanus*) with the description of a fossil black bear from Bill Neff Cave, Virginia. *Illinois State Museum Scientific Papers* 23:238-250.

- Graham R, Lundelius E Jr. 2010. FAUNMAP II: new data for North America with a temporal extension for the Blancan, Irvingtonian and early Rancholabrean. FAUNMAP II Database, version 1.
- Guilday, J.E. 1968. Grizzly bears from eastern North America. *American Midland Naturalist*:247-250.
- Guilday JE, Parmalee PW, Hamilton HW. 1977. The Clark's Cave bone deposit and the late Pleistocene paleoecology of the central Appalachian Mountains of Virginia.
- Kurtén B, Anderson E. 1980. Pleistocene mammals of North America. Columbia University Press.
- Kurtén, J. 1963. Fossil bears from Texas. *The Pearce-Sellards Series* 1:3-14
- Kutschera VE, Bidon T, Hailer F, Rodi JL, Fain SR, Janke A. 2014. Bears in a forest of gene trees: phylogenetic inference is complicated by incomplete lineage sorting and gene flow. *Molecular biology and evolution* 31(8):2004-2017.
- Larivière, S. 2001. *Ursus americanus*. *Mammalian species* 647:1-11.
- Matheus, P.E. 1995. Diet and co-ecology of Pleistocene short-faced bears and brown bears in eastern Beringia. *Quaternary Research* 44(3):447-453.
- Matheus P, Burns J, Weinstock J, Hofreiter M. 2004. Pleistocene brown bears in the mid-continent of North America. *Science* 306(5699):1150.

- Meachen JA, Brannick AL, Fry TJ. 2016. Extinct Beringian wolf morphotype found in the continental US has implications for wolf migration and evolution. *Ecology and Evolution*.
- Meloro, C. 2011. Feeding habits of Plio-Pleistocene large carnivores as revealed by the mandibular geometry. *Journal of Vertebrate Paleontology* 31(2):428-446.
- Mustoe GE, Carlstad CA. 1995. A late Pleistocene brown bear (*Ursus arctos*) from northwest Washington. *Northwest Science* 69(2):106-113
- Pasitschniak-Arts, M. 1993. *Ursus arctos*. *Mammalian Species* 439:1-10.
- Pelton MR, Coley AB, Eason TH, Martinez DD, Pederson JA, van Manen FT, Weaver KM, SERVHEEN Y. 1999. American black bear conservation action plan. C.Servheen, S.Herrero, and B.Peyton, compilers. *Bears. Status survey and conservation action plan. IUCN/SSC bear and polar bear specialist groups*. 144-156.
- Rohlf, F.J. 2015. The tps series of software. *Hystrix, the Italian Journal of Mammalogy* 26(1):9-12.
- Sorkin, B. 2006. Ecomorphology of the giant short-faced bears *Agriotherium* and *Arctodus*. *Historical Biology* 18(1):1-20.
- Taberlet P, Bouvet J. 1994. Mitochondrial DNA polymorphism, phylogeography, and conservation genetics of the brown bear *Ursus arctos* in Europe. *Proceedings. Biological sciences* 255(1344):195-200.

Wolverton S, Lyman RL. 1998. Measuring late Quaternary ursid diminution in the Midwest. *Quaternary Research* 49(3):322-329.

APPENDIX

Additional Tables and Figures

Specimen	Species	State or Territory
USNM 236227	<i>U. americanus</i>	Colorado
USNM 224509	<i>U. americanus</i>	Colorado
USNM 223943	<i>U. americanus</i>	Florida
USNM 234242	<i>U. americanus</i>	Florida
USNM 227660	<i>U. americanus</i>	Idaho
USNM 216420	<i>U. americanus</i>	Idaho
USNM A03061	<i>U. americanus</i>	New York
USNM 187876	<i>U. americanus</i>	New York
USNM 228262	<i>U. americanus</i>	New Mexico
USNM 231359	<i>U. americanus</i>	New Mexico
USNM 206132	<i>U. americanus</i>	Alaska
USNM 087617	<i>U. americanus</i>	British Colombia
USNM 081198	<i>U. americanus</i>	Quebec
USNM 205950	<i>U. americanus</i>	California
USNM 248531	<i>U. americanus</i>	Washington
USNM 159368	<i>U. americanus</i>	Louisiana
USNM 135141	<i>U. americanus</i>	Louisiana
USNM 227926	<i>U. americanus</i>	Wyoming
ETVP 18252	<i>U. americanus</i>	Tennessee
ETVP 18244	<i>U. americanus</i>	Tennessee
ETVP 7170	<i>U. americanus</i>	Tennessee
ETVP 7169	<i>U. americanus</i>	Quebec
ETVP 5011	<i>U. americanus</i>	?
ETVP 18233	<i>U. americanus</i>	Tennessee
NAUQSP 7607	<i>U. americanus</i>	Maine
CC.279	<i>U. americanus</i>	?
CC.388	<i>U. americanus</i>	?
NVPL 6918	<i>U. americanus</i>	Tennessee
ETVP 7173	<i>U. americanus</i>	?
ETVP 10138	<i>U. americanus</i>	Tennessee
ETVP 7179	<i>U. americanus</i>	?
ETVP 10129	<i>U. americanus</i>	Tennessee
ETVP 10139	<i>U. americanus</i>	Tennessee
ETVP 18175	<i>U. americanus</i>	Tennessee
USNM 211240	<i>U. arctos</i>	Montana

USNM 225621	<i>U. arctos</i>	Montana
USNM 098324	<i>U. arctos</i>	Chihuahua
USNM 098320	<i>U. arctos</i>	Chihuahua
USNM A31276	<i>U. arctos</i>	Idaho
USNM 233241	<i>U. arctos</i>	Idaho
USNM 113410	<i>U. arctos</i>	Colorado
USNM 113411	<i>U. arctos</i>	Colorado
USNM 228228	<i>U. arctos</i>	Yukon
USNM 227977	<i>U. arctos</i>	Yukon
USNM 223945	<i>U. arctos</i>	British Colombia
USNM 223689	<i>U. arctos</i>	British Colombia
USNM 262374	<i>U. arctos</i>	New Mexico
USNM 223034	<i>U. arctos</i>	Utah
USNM 228226	<i>U. arctos</i>	California
USNM 235445	<i>U. arctos</i>	Wyoming
USNM 203524	<i>U. arctos</i>	North Dakota
USNM 242652	<i>U. arctos</i>	Arizona
USNM 243786	<i>U. arctos</i>	Washington
USNM 222107	<i>U. arctos</i>	Alberta
ETVP 5162	<i>U. arctos</i>	?
ETVP 18264	<i>U. arctos</i>	Alaska
AKGBR 9904282	<i>U. arctos</i>	Alaska
AKGBR 0304553	<i>U. arctos</i>	Alaska
AKGBR 0502474	<i>U. arctos</i>	Alaska
AKGBR 1002343	<i>U. arctos</i>	Alaska
AHGBR 0304912	<i>U. arctos</i>	Alaska
AKGBR	<i>U. arctos</i>	Alaska
ETVP 10145	<i>U. arctos</i>	?
ETVP 10501	<i>U. arctos</i>	?

Casewise Statistics

Case Number	Actual Group	Highest Group					Second Highest Group			Discriminant Scores
		Predicted Group	P(D>d G=g)		P(G=g D=d)	Squared Mahalanobis Distance to Centroid	Group	P(G=g D=d)	Squared Mahalanobis Distance to Centroid	Function 1
			p	df						
Original 1	1	1	.599	1	1.000	.277	2	.000	28.125	-2.206
2	1	1	.868	1	1.000	.028	2	.000	32.078	-2.567
3	1	1	.998	1	1.000	.000	2	.000	33.952	-2.730
4	1	1	.718	1	1.000	.130	2	.000	29.906	-2.372
5	1	1	.994	1	1.000	.000	2	.000	34.079	-2.741
6	1	1	.719	1	1.000	.130	2	.000	29.913	-2.372
7	1	1	.841	1	1.000	.040	2	.000	31.692	-2.533
8	1	1	.603	1	1.000	.271	2	.000	40.327	-3.253
9	1	1	.085	1	1.000	2.966	2	.000	57.031	-4.455
10	1	1	.862	1	1.000	.030	2	.000	31.994	-2.559
11	1	1	.031	1	.988	4.660	2	.012	13.476	-.574
12	1	1	.895	1	1.000	.018	2	.000	35.547	-2.865
13	1	1	.499	1	1.000	.457	2	.000	42.319	-3.408
14	1	1	.710	1	1.000	.138	2	.000	38.452	-3.104
15	1	1	.167	1	1.000	1.910	2	.000	19.781	-1.351
16	1	1	.178	1	1.000	1.812	2	.000	51.490	-4.079
17	1	1	.861	1	1.000	.031	2	.000	31.976	-2.558
18	1	1	.925	1	1.000	.009	2	.000	35.092	-2.827
19	2	2	.717	1	1.000	.131	1	.000	38.335	3.459
20	2	2	.329	1	1.000	.951	1	.000	46.307	4.072
21	2	2	.477	1	1.000	.506	1	.000	42.789	3.809
22	2	2	.585	1	1.000	.299	1	.000	40.658	3.644
23	2	2	.221	1	1.000	1.498	1	.000	21.212	1.873
24	2	2	.988	1	1.000	.000	1	.000	34.163	3.112
25	2	2	.670	1	1.000	.182	1	.000	39.134	3.523
26	2	2	.580	1	1.000	.306	1	.000	27.843	2.544
27	2	2	.116	1	1.000	2.471	1	.000	18.127	1.525
28	2	2	.203	1	1.000	1.621	1	.000	20.760	1.824
29	2	2	.253	1	1.000	1.305	1	.000	48.610	4.239
30	2	2	.406	1	1.000	.691	1	.000	24.986	2.266
31	2	2	.620	1	1.000	.246	1	.000	40.010	3.593
32	2	2	.401	1	1.000	.704	1	.000	44.471	3.936
33	2	2	.283	1	1.000	1.153	1	.000	47.655	4.171
34	2	2	.079	1	1.000	3.080	1	.000	57.525	4.852
35	2	2	.991	1	1.000	.000	1	.000	33.856	3.086
36	2	2	.797	1	1.000	.066	1	.000	31.058	2.840
37	2	2	.433	1	1.000	.615	1	.000	25.455	2.313
38	2	2	.654	1	1.000	.201	1	.000	39.414	3.545
39	1	1	.449	1	1.000	.573	2	.000	43.386	-3.490
40	1	1	.396	1	1.000	.722	2	.000	44.612	-3.582
41	1	1	.959	1	1.000	.003	2	.000	34.589	-2.784
42	1	1	.363	1	1.000	.826	2	.000	24.215	-1.824
43	1	1	.031	1	1.000	4.662	2	.000	63.820	-4.892
44	1	1	.289	1	1.000	1.123	2	.000	22.752	-1.673
45	1	1	.328	1	1.000	.958	2	.000	46.355	-3.711
46	1	1	.824	1	1.000	.050	2	.000	31.439	-2.510
47	1	1	.586	1	1.000	.297	2	.000	27.928	-2.188
48	1	1	.188	1	1.000	1.730	2	.000	20.379	-1.417
49	1	1	.775	1	1.000	.082	2	.000	37.406	-3.019
50	1	1	.044	1	.995	4.075	2	.005	14.523	-.714
51	1	1	.541	1	1.000	.373	2	.000	41.482	-3.344
52	1	1	.334	1	1.000	.934	2	.000	46.188	-3.699
53	1	1	.095	1	1.000	2.788	2	.000	56.242	-4.402
54	1	1	.104	1	.999	2.640	2	.001	17.681	-1.108
55	2	2	.007	1	.762	7.371	1	.238	9.701	.382
56	2	2	.923	1	1.000	.009	1	.000	32.867	3.000
57	2	2	.753	1	1.000	.099	1	.000	30.422	2.783
58	2	2	.952	1	1.000	.004	1	.000	33.285	3.037
59	2	2	.906	1	1.000	.014	1	.000	35.381	3.216
60	2	2	.127	1	1.000	2.329	1	.000	54.109	4.623
61	2	2	.479	1	1.000	.500	1	.000	42.733	3.804
62	2	2	.797	1	1.000	.066	1	.000	31.047	2.839
63	2	2	.731	1	1.000	.119	1	.000	30.088	2.753
64	2	2	.396	1	1.000	.721	1	.000	24.804	2.248

Cross-validated ^b	1	1	1	.001	22	1.000	47.831	2	.000	68.134
	2	1	1	.020	22	1.000	37.657	2	.000	65.893
	3	1	1	.281	22	1.000	25.335	2	.000	57.258
	4	1	1	.060	22	1.000	33.160	2	.000	58.459
	5	1	1	.642	22	1.000	19.052	2	.000	51.504
	6	1	1	.000	22	1.000	74.153	2	.000	94.437
	7	1	1	.131	22	1.000	29.517	2	.000	57.902
	8	1	1	.430	22	1.000	22.512	2	.000	62.960
	9	1	1	.000	22	1.000	76.113	2	.000	152.465
	10	1	1	.086	22	1.000	31.497	2	.000	60.149
	11	1	2**	.000	22	1.000	63.897	1	.000	89.324
	12	1	1	.000	22	1.000	78.147	2	.000	110.486
	13	1	1	.000	22	1.000	55.021	2	.000	100.281
	14	1	1	.403	22	1.000	22.986	2	.000	61.012
	15	1	1	.319	22	.997	24.552	2	.003	35.994
	16	1	1	.035	22	1.000	35.396	2	.000	92.490
	17	1	1	.001	22	1.000	48.515	2	.000	75.615
	18	1	1	.746	22	1.000	17.309	2	.000	51.127
	19	2	2	.833	22	1.000	15.639	1	.000	53.322
	20	2	2	.002	22	1.000	45.509	1	.000	96.132
	21	2	2	.016	22	1.000	38.483	1	.000	82.994
	22	2	2	.595	22	1.000	19.805	1	.000	60.402
	23	2	2	.120	22	.998	29.933	1	.002	41.938
	24	2	2	.006	22	1.000	42.022	1	.000	72.995
	25	2	2	.057	22	1.000	33.332	1	.000	72.207
	26	2	2	.000	22	.974	122.697	1	.026	129.913
	27	2	1**	.000	22	.650	53.449	2	.350	54.684
	28	2	2	.423	22	.999	22.628	1	.001	35.966
	29	2	2	.002	22	1.000	45.274	1	.000	99.501
	30	2	2	.008	22	1.000	41.279	1	.000	56.877
	31	2	2	.003	22	1.000	44.501	1	.000	84.950
	32	2	2	.010	22	1.000	40.231	1	.000	87.434
	33	2	2	.981	22	1.000	10.511	1	.000	58.375
	34	2	2	.001	22	1.000	48.420	1	.000	117.296
	35	2	2	.013	22	1.000	39.372	1	.000	70.022
	36	2	2	.000	22	1.000	75.640	1	.000	97.725
	37	2	2	.428	22	1.000	22.545	1	.000	42.758
	38	2	2	.075	22	1.000	32.116	1	.000	71.377
	39	1	1	.946	22	1.000	12.516	2	.000	56.024
	40	1	1	.866	22	1.000	14.901	2	.000	60.026
	41	1	1	1.000	22	1.000	6.066	2	.000	39.801
	42	1	1	.001	22	.998	49.116	2	.002	61.952
	43	1	1	.000	22	1.000	57.199	2	.000	139.577
	44	1	1	.835	22	1.000	15.612	2	.000	33.746
	45	1	1	.078	22	1.000	31.988	2	.000	81.317
	46	1	1	.000	22	1.000	51.260	2	.000	77.139
	47	1	1	.053	22	1.000	33.691	2	.000	55.826
	48	1	1	.079	22	.994	31.892	2	.006	42.185
	49	1	1	.008	22	1.000	41.152	2	.000	77.715
	50	1	2**	.072	22	.514	32.306	1	.486	32.418
	51	1	1	.504	22	1.000	21.268	2	.000	63.130
	52	1	1	.001	22	1.000	47.797	2	.000	98.897
	53	1	1	.342	22	1.000	24.095	2	.000	84.778
	54	1	1	.309	22	.983	24.754	2	.017	32.821
	55	2	1**	.041	22	1.000	34.757	2	.000	56.026
	56	2	2	.830	22	1.000	15.711	1	.000	46.739
	57	2	2	.000	22	1.000	52.491	1	.000	75.989
	58	2	2	.000	22	1.000	57.580	1	.000	85.923
	59	2	2	.113	22	1.000	30.221	1	.000	63.700
	60	2	2	.000	22	1.000	52.336	1	.000	116.748
	61	2	2	.708	22	1.000	17.974	1	.000	61.016
	62	2	2	.288	22	1.000	25.181	1	.000	52.883
	63	2	2	.303	22	1.000	24.887	1	.000	51.275
	64	2	2	.387	22	1.000	23.270	1	.000	42.398

For the original data, squared Mahalanobis distance is based on canonical functions.

For the cross-validated data, squared Mahalanobis distance is based on observations.

** Misclassified case

b. Cross validation is done only for those cases in the analysis. In cross validation, each case is classified by the functions derived from all cases other than that case.

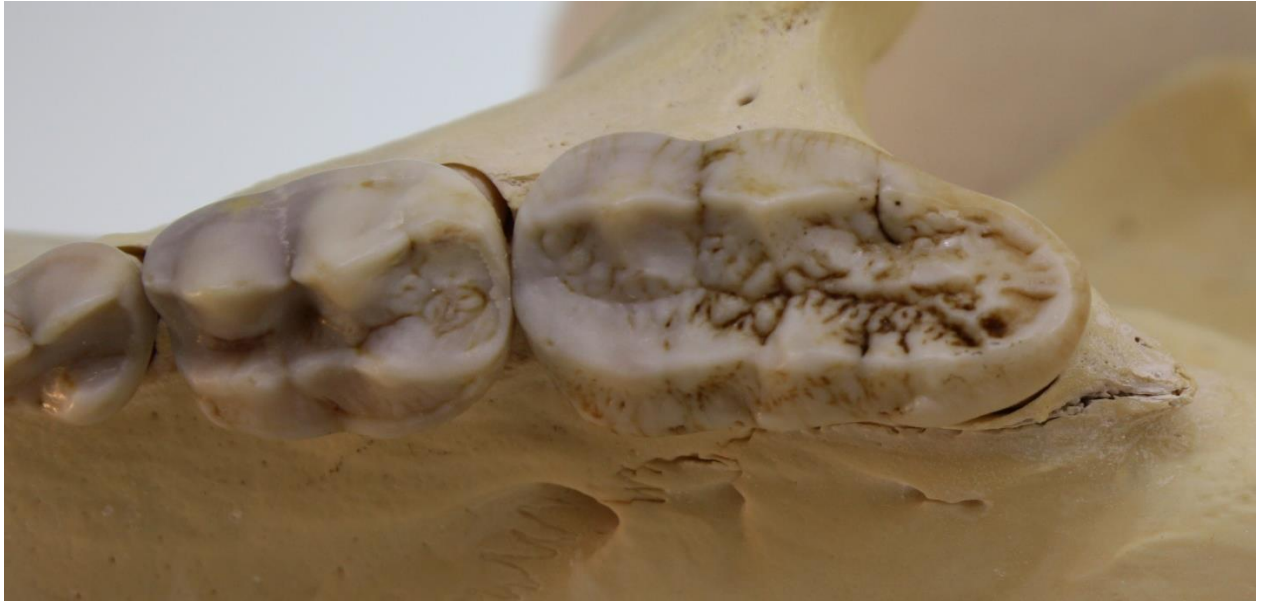
Misidentified Specimens



USNM 206132



USNM 228228



ETVP 10138



ETVP 5162 (Believed to actually be misidentified, and should be assigned to U. americanus)

Carnegie Specimens



CM 12617



CM 12999

Case Study Casewise Statistics

Casewise Statistics												
Case Number	Actual Group	Predicted Group	Highest Group					Second Highest Group			Discriminant Scores	
			P(D>d G=g)		P(G=g D=d)	Squared Mahalanobis Distance to Centroid	Group	P(G=g D=d)	Squared Mahalanobis Distance to Centroid	Function 1		
			p	df								
Original	1	1	.572	1	1.000	.320	2	.000	27.532	-2.159		
	2	1	.879	1	1.000	.023	2	.000	32.044	-2.573		
	3	1	.955	1	1.000	.003	2	.000	33.133	-2.668		
	4	1	.734	1	1.000	.115	2	.000	29.960	-2.385		
	5	1	.995	1	1.000	.000	2	.000	33.720	-2.719		
	6	1	.704	1	1.000	.144	2	.000	29.521	-2.345		
	7	1	.891	1	1.000	.019	2	.000	32.218	-2.588		
	8	1	.616	1	1.000	.252	2	.000	39.877	-3.227		
	9	1	.085	1	1.000	2.959	2	.000	56.748	-4.445		
	10	1	.947	1	1.000	.004	2	.000	33.020	-2.658		
	11	1	.033	1	.989	4.522	2	.011	13.590	-.598		
	12	1	.940	1	1.000	.006	2	.000	34.672	-2.800		
	13	1	.470	1	1.000	.523	2	.000	42.717	-3.448		
	14	1	.722	1	1.000	.127	2	.000	38.052	-3.081		
	15	1	.146	1	1.000	2.118	2	.000	18.988	-1.269		
	16	1	.207	1	1.000	1.592	2	.000	50.048	-3.986		
	17	1	.978	1	1.000	.001	2	.000	34.116	-2.753		
	18	1	.915	1	1.000	.011	2	.000	35.034	-2.831		
	19	2	.716	1	1.000	.133	1	.000	38.157	3.452		
	20	2	.318	1	1.000	.995	1	.000	46.383	4.086		
	21	2	.525	1	1.000	.405	1	.000	41.593	3.724		
	22	2	.566	1	1.000	.329	1	.000	40.787	3.662		
	23	2	.204	1	1.000	1.615	1	.000	20.630	1.817		
	24	2	.986	1	1.000	.000	1	.000	33.583	3.070		
	25	2	.724	1	1.000	.125	1	.000	38.023	3.441		
	26	2	.620	1	1.000	.246	1	.000	28.274	2.593		
	27	2	.123	1	1.000	2.374	1	.000	18.250	1.547		
	28	2	.222	1	1.000	1.494	1	.000	21.073	1.866		
	29	2	.240	1	1.000	1.382	1	.000	48.837	4.264		
	30	2	.382	1	1.000	.765	1	.000	24.388	2.214		
	31	2	.683	1	1.000	.167	1	.000	38.705	3.497		
	32	2	.330	1	1.000	.949	1	.000	46.065	4.062		
	33	2	.274	1	1.000	1.199	1	.000	47.717	4.183		
	34	2	.067	1	1.000	3.351	1	.000	58.423	4.919		
	35	2	.992	1	1.000	.000	1	.000	33.676	3.078		
	36	2	.794	1	1.000	.068	1	.000	30.924	2.827		
	37	2	.457	1	1.000	.553	1	.000	25.695	2.344		
	38	2	.675	1	1.000	.176	1	.000	38.836	3.507		
	39	1	.451	1	1.000	.569	2	.000	43.129	-3.479		
	40	1	.382	1	1.000	.763	2	.000	44.707	-3.598		
	41	1	.969	1	1.000	.002	2	.000	34.243	-2.764		
	42	1	.348	1	1.000	.880	2	.000	23.765	-1.787		
	43	1	.035	1	1.000	4.422	2	.000	62.658	-4.828		
	44	1	.333	1	1.000	.935	2	.000	23.481	-1.758		
	45	1	.320	1	1.000	.988	2	.000	46.336	-3.719		
	46	1	.925	1	1.000	.009	2	.000	32.698	-2.630		
	47	1	.535	1	1.000	.386	2	.000	26.955	-2.104		
	48	1	.177	1	1.000	1.822	2	.000	19.920	-1.375		
	49	1	.879	1	1.000	.023	2	.000	35.585	-2.877		
	50	1	.048	1	.996	3.894	2	.004	14.742	-.751		
	51	1	.504	1	1.000	.446	2	.000	42.001	-3.393		
	52	1	.406	1	1.000	.689	2	.000	44.129	-3.555		
	53	1	.093	1	1.000	2.817	2	.000	56.120	-4.403		
	54	1	.102	1	.999	2.680	2	.001	17.437	-1.088		
	55	2	.006	1	.715	7.553	1	.285	9.392	.340		
	56	2	.919	1	1.000	.010	1	.000	32.622	2.987		
	57	2	.729	1	1.000	.120	1	.000	29.884	2.742		
	58	2	.927	1	1.000	.008	1	.000	32.730	2.996		
	59	2	.920	1	1.000	.010	1	.000	34.971	3.189		
	60	2	.118	1	1.000	2.447	1	.000	54.421	4.652		
	61	2	.460	1	1.000	.546	1	.000	42.922	3.827		
	62	2	.755	1	1.000	.097	1	.000	30.262	2.776		
	63	2	.712	1	1.000	.137	1	.000	29.628	2.718		
	64	2	.408	1	1.000	.683	1	.000	24.863	2.261		
	65	ungrouped	.131	1	1.000	2.276	1	.000	18.527	1.579		
	66	ungrouped	.453	1	1.000	.564	2	.000	43.086	-3.476		

Cross-validated ^b	1	1	.001	22	1.000	47.835	2	.000	67.223
2	1	1	.019	22	1.000	37.894	2	.000	66.173
3	1	1	.278	22	1.000	25.417	2	.000	56.280
4	1	1	.062	22	1.000	32.999	2	.000	58.509
5	1	1	.620	22	1.000	19.412	2	.000	51.443
6	1	1	.000	22	1.000	82.439	2	.000	101.053
7	1	1	.106	22	1.000	30.554	2	.000	59.718
8	1	1	.412	22	1.000	22.815	2	.000	62.753
9	1	1	.000	22	1.000	74.834	2	.000	150.427
10	1	1	.065	22	1.000	32.789	2	.000	62.978
11	1	2**	.000	22	1.000	63.240	1	.000	87.125
12	1	1	.000	22	1.000	76.293	2	.000	107.033
13	1	1	.000	22	1.000	56.451	2	.000	102.669
14	1	1	.401	22	1.000	23.017	2	.000	60.583
15	1	1	.362	22	.995	23.720	2	.005	34.273
16	1	1	.055	22	1.000	33.536	2	.000	88.316
17	1	1	.008	22	1.000	41.201	2	.000	72.589
18	1	1	.719	22	1.000	17.784	2	.000	51.563
19	2	2	.817	22	1.000	15.983	1	.000	53.494
20	2	2	.003	22	1.000	45.191	1	.000	96.004
21	2	2	.026	22	1.000	36.564	1	.000	79.263
22	2	2	.611	22	1.000	19.548	1	.000	60.343
23	2	2	.163	22	.997	28.396	1	.003	40.002
24	2	2	.004	22	1.000	43.602	1	.000	73.645
25	2	2	.061	22	1.000	33.057	1	.000	70.400
26	2	2	.000	22	.985	126.566	1	.015	134.888
27	2	1**	.000	22	.562	53.323	2	.438	53.823
28	2	2	.559	22	.999	20.391	1	.001	34.896
29	2	2	.002	22	1.000	46.182	1	.000	101.012
30	2	2	.009	22	.999	40.765	1	.001	55.572
31	2	2	.002	22	1.000	45.259	1	.000	83.718
32	2	2	.008	22	1.000	41.004	1	.000	90.815
33	2	2	.981	22	1.000	10.544	1	.000	58.489
34	2	2	.000	22	1.000	51.879	1	.000	123.263
35	2	2	.006	22	1.000	41.999	1	.000	72.304
36	2	2	.000	22	1.000	77.637	1	.000	99.219
37	2	2	.436	22	1.000	22.404	1	.000	43.067
38	2	2	.054	22	1.000	33.569	1	.000	72.104
39	1	1	.948	22	1.000	12.421	2	.000	55.656
40	1	1	.885	22	1.000	14.449	2	.000	59.662
41	1	1	1.000	22	1.000	6.231	2	.000	39.605
42	1	1	.001	22	.998	49.098	2	.002	61.252
43	1	1	.000	22	1.000	61.056	2	.000	142.996
44	1	1	.859	22	1.000	15.064	2	.000	34.361
45	1	1	.072	22	1.000	32.329	2	.000	81.748
46	1	1	.001	22	1.000	49.236	2	.000	77.706
47	1	1	.069	22	1.000	32.498	2	.000	53.405
48	1	1	.080	22	.992	31.876	2	.008	41.522
49	1	1	.006	22	1.000	42.399	2	.000	76.128
50	1	1	.078	22	.574	31.945	2	.426	32.539
51	1	1	.559	22	1.000	20.385	2	.000	62.893
52	1	1	.001	22	1.000	47.098	2	.000	94.890
53	1	1	.350	22	1.000	23.951	2	.000	84.472
54	1	1	.296	22	.979	25.016	2	.021	32.702
55	2	1**	.058	22	1.000	33.281	2	.000	54.274
56	2	2	.787	22	1.000	16.572	1	.000	47.274
57	2	2	.000	22	1.000	51.166	1	.000	74.006
58	2	2	.000	22	1.000	56.563	1	.000	84.116
59	2	2	.105	22	1.000	30.565	1	.000	63.524
60	2	2	.000	22	1.000	53.350	1	.000	118.620
61	2	2	.722	22	1.000	17.736	1	.000	61.028
62	2	2	.266	22	1.000	25.668	1	.000	52.289
63	2	2	.273	22	1.000	25.507	1	.000	51.248
64	2	2	.379	22	1.000	23.403	1	.000	42.672

For the original data, squared Mahalanobis distance is based on canonical functions.

For the cross-validated data, squared Mahalanobis distance is based on observations.

** Misclassified case

b. Cross validation is done only for those cases in the analysis. In cross validation, each case is classified by the functions derived from all cases other than that case.

VITA

THERON MICHAEL KANTELIS

Education: North Forsyth High School, Cumming, Georgia 2011
B.S. Biology, Berry College, Mount Berry, Georgia 2015
M.S. Geosciences, East Tennessee State University,
Johnson City, Tennessee 2017

Professional Experience: Graduate Assistant, East Tennessee State University,
Department of Geosciences, 2015-2017